

國立交通大學

光電工程研究所

碩士論文

多重性能之光學薄膜應用於高效率背光模組

A Multi-Performance Film for Highly Efficient LCD
Backlights



研究生：謝仁杰

指導教授：謝漢萍 教授
黃乙白 助理教授

中華民國 九十七 年 七 月

多重性能之光學薄膜應用於高效率背光模組

A Multi-Performance Film for Highly Efficient LCD Backlights

研究生：謝仁杰
指導教授：謝漢萍
黃乙白

Student : Jen-Chieh Hsieh
Advisor : Han-Ping D. Shieh
Yi-Pai Huang



Submitted to Institute of Electro-Optical Engineering
College of Electrical Engineering
National Chiao-Tung University
in Partial Fulfillment of the Requirements
for the Degree of
Master
in

Electro-Optical Engineering

July 2008

Hsinchu, Taiwan, Republic of China

中華民國九十七年七月

多重性能薄膜應用於高效率背光模組

碩士研究生：謝仁杰

指導教授：謝漢萍 教授

黃乙白 助理教授

國立交通大學

光電工程研究所

摘 要

液晶電視(LCD-TV)與傳統陰極射線管電視相比，其具有高解析度、低功率、輕薄等優點，可以提供較佳的影像品質。直下式背光系統是目前的主要趨勢用來提供液晶電視的足夠亮度光源。然而，這種背光系統卻面臨了高價格和亮度不均勻(lamp-Mura)等問題。為了改善這些問題，本論文提出一種新型的光學薄膜，成功地有效提升背光系統的效能，並且減少其光學薄膜成本。

與傳統的增光膜(brightness enhancement film)比較，本論文提出的新式光學薄膜，「多重效能薄膜(Multi-Performance Film, MPF)」，在表面上具有凹狀拋物面稜鏡結構，因而同時具有增光和散射的特性。藉由模擬和實驗結果，MPF 成功地消除 lamp-Mura 並且增加背光系統的亮度視角及光輸出效率。

然而，當進一步降低背光系統的厚度時，MPF 在消除 lamp-Mura 有其極限。因此，本論文藉由「非均勻多重效能薄膜(Patterned-MPF)」來改善薄型化背光系統的 lamp-Mura。Patterned-MPF 乃是對應距離燈管不同位置對凹狀拋物面稜鏡的曲率進行優化。經由模擬結果驗證，薄型化背光系統的確產生均勻的光場輸出，並且有效地消除 lamp-Mura。

A Multi-Performance Film for Highly Efficient LCD Backlights

Master Student: Jen-Chieh Hsieh

**Advisor: Dr. Han-Ping D. Shieh
Dr. Yi-Pai Huang**

**Institute of Electro-Optical Engineering
National Chiao Tung University**

Abstract

Liquid crystal display TVs (LCD-TVs) have advantages, such as high definition, low power-consumption, and light weight, etc, which can produce a higher quality image. Direct-emitting backlight systems are needed to provide a sufficiently bright and uniform light source for LCD-TVs. However, the direct-emitting backlight system has some issues, such as high cost and lamp-Mura defect. Thus, a novel optical film is proposed to resolve these issues in this thesis.

Compared with a conventional brightness enhancement film (BEF), the proposed multi-performance film (MPF) includes concave-parabolic prism structures on the surface. Thus, the MPF can integrate the brightness enhancement and light scattering functions simultaneously. According to the simulation and experimental results, MPF successfully suppressed lamp-Mura and enhanced the optical performance in backlight systems.

When the backlight thickness is reduced, MPFs have a limited capability to suppress lamp-Mura. Therefore, a Patterned-MPF modified from the original MPF is designed to suppress lamp-Mura in a slim backlight system. The Patterned-MPF has optimized prism profile curvatures depended on the position from lamps. From simulation results, a slim backlight system with a uniform light output was achieved.

誌 謝

首先，我要感謝謝漢萍教授和黃乙白教授這兩年來在研究上、表達能力上與生活細節上的細心指導，並提供了完備的研究環境，使我能專心於平面顯示器技術的研究，並且有機會能到國外參加國際級的研討會，開拓視野。也因此能順利完成碩士論文。

在研究上，首先我要感謝陳均合學長常常給予我建議和提醒，讓我能順利完成研究，其次，還要感謝方仁宇和羅友群學長在研究初期給予細心的指導和教學。此外，我要感謝劉康仲學長和奇新科技公司的余谷聲、吳詩斌和廖致力前輩們在實驗上的協助與支持，使我能順利完成實驗。

在這兩年裡，我很感激與我一起奮鬥的同學們，國振、明農、其霖、景明、宛徵、建良、勝昌，以及其他實驗室的夥伴們，和你們一起時所擁有的歡笑和辛酸，是我碩士生涯裡難忘的記憶。另外，我很高興能與楊柏儒、林坤岳和呂健嘉學長們一起參與奇美獎競賽，與你們在一起讓我學習到很多。實驗室裡的其他學長姐們，鄭榮安、李企恒、鄭裕國、莊喬舜、林芳正、許精益等等，以及已畢業的學長姐，也非常感謝你們的平日的照顧和關心。還有碩一和大學部專題生的學弟妹們，我也要感謝你們平日的幫忙以及帶給了實驗室歡樂。此外，雅惠、偉誠和其他諸位漂亮的所辦小姐們，我也要謝謝你們這兩年來對我的照顧和幫忙。當然，我還要感謝關心我的朋友和死黨們，因為有你們在，讓我碩士生活增加了不少樂趣。

最後，我要將這篇碩士論文獻給我最摯愛的父母親、爺爺和奶奶，因為你們不辭辛勞的付出與關心，讓我無所顧慮地順利完成學業並長成至今。也因為有你們的教導，讓我在做人處事上都能順順利利。在未來的日子裡我必當竭盡所能來報答你們、孝順你們。謝謝我的家人對我所付出的一切，讓我在此致上我最誠摯的感謝。

Table of Contents

Abstract (Chinese).....	i
Abstract (English).....	ii
Acknowledgement.....	iii
Table of Contents	iv
Figure Captions	vi
List of Tables.....	viii
Chapter 1 Introduction.....	1
1.1 Liquid crystal displays (LCDs).....	1
1.2 Direct-emitting backlight systems.....	2
1.3 Lamp-Mura issue.....	4
1.4 Motivation and objectives.....	6
1.5 Organization of this Thesis.....	7
Chapter 2 Principles of backlight system.....	8
2.1 Ray-tracing method.....	8
2.2 Lamp-Mura contrast.....	11
2.3 Bidirectional scatter distribution function (BSDF).....	12
2.4 Principle of brightness enhancement film (BEF).....	14
2.5 Summary.....	18
Chapter 3 Design and simulation of MPF.....	19
3.1 Design of MPF.....	19
3.2 Experiment backlight structures.....	21
3.3 Specification of demonstrated backlight system.....	22
3.4 Simulation models.....	24
3.5 Simulation results.....	25
3.5.1 Lamp-Mura contrast and optimized curvature.....	26
3.5.2 Average luminance.....	27
3.6 Summary.....	28
Chapter 4 Fabrication technologies and measurement instruments.....	29

4.1	Screen printing process of MPFs.....	29
4.2	Measurement instruments.....	30
4.2.1	Conoscopic system.....	31
4.2.2	BTDF measurement device.....	32
4.3	Summary.....	33
Chapter 5 Experimental results and discussions		34
5.1	Fabrication results	34
5.2	Experimental results	36
5.2.1	Lamp-Mura contrast and average luminance of MPF case.....	36
5.2.2	Normal brightness and viewing angle.....	38
5.2.3	Relative output light efficiency.....	39
5.2.4	Real luminance images.....	40
5.3	Summary and discussion.....	41
Chapter 6 Patterned-MPF.....		44
6.1	Design and simulation results.....	45
6.2	Summary.....	49
Chapter 7 Conclusions and future work.....		50
7.1	Multi-performance film for suppressing lamp-Mura.....	50
7.2	Patterned multi-performance film for slim backlight systems	52
7.3	Future work	53
Reference.....		54

Figure Captions

Fig. 1-1 Schematic of a liquid crystal display.	2
Fig. 1-2 Schematic configuration of a direct-emitting backlight system.	3
Fig. 1-3 The ratio of the backlight cost of (a) 15-inch side-emitting and (b) 30-inch direct-emitting backlight in the LCD [□]	4
Fig. 1-4 Lamp-Mura captured by a charge-coupled device (CCD).....	5
Fig. 2-1 Diagram of lamp-Mura.	12
Fig. 2-2 Schematic of BSDF.	13
Fig. 2-3 Diagram of BEF working principle [□]	15
Fig. 2-4 Diagram of the angular distribution using BEF III, where the black line is without any BEF; the blue line added a BEF; and the red line placed two BEFs crossed at 90°.....	15
Fig. 2-5 Schematics of the backlight luminance distribution (a) without and (b) with a BEF, and (c) measurement results.....	17
Fig. 2-6 Schematic of ray-tracing in a BEF.....	17
Fig. 3-1 Schematic of MPFs.....	20
Fig. 3-2 Ray-tracing diagrams of (a) conventional BEF and (b) MPF.....	21
Fig. 3-3 Schematic of backlight luminance distribution by using a MPF.....	21
Fig. 3-4 Schematics of experiment backlight structures.....	22
Fig. 3-5 Demonstration of a 32-inch backlight system.	23
Fig. 3-6 Measured BTDFs of the (a) top diffuser, (b) bottom diffuser, and (c) diffusive plate, and BRDF of the (d) reflector.	25
Fig. 3-7 Luminance distributions of (a) MPF case and (b) MPF-Plate case, where C is curvature.	26
Fig. 3-8 Lamp-Mura contrast of MPF and MPF-Plate case.	27
Fig. 3-9 Average luminance of MPF and MPF-Plate case.....	27
Fig. 4-1 Schematic of screen printing process.....	30
Fig. 4-2 Schematic of used BEF structure.....	30
Fig. 4-3 Schematic of the conoscopic system in transmissive mode.....	31
Fig. 4-4 Schematic of our designed device for BTDF measurement.	32
Fig. 4-5 Diagram of BTDF measurement.....	33
Fig. 5-1 Measured MPF surface profiles.....	35
Fig. 5-2 Fitting profiles of filling ratio (a) 10% and (b) 25% MPFs.....	35
Fig. 5-3 Relationship between filling ratio and curvature.....	36

Fig. 5-4 Measured luminance distributions of conventional backlight and MPF case.....	37
Fig. 5-5 Comparisons of simulation and experimental results in the MPF case, (a) lamp-Mura contrast and (b) relative average luminance.	38
Fig. 5-6 Diagrams of luminance cross-section in (a) horizontal and (b) vertical.....	39
Fig. 5-7 Diagrams of angular luminance contour, (a) the conventional backlight, (b) MPF case, and (c) MPF-Plate case.	40
Fig. 5-8 Captured results by a CCD camera, the captured size on the backlight is 20cm by 20cm.	41
Fig. 5-9 OM pictures of filling ratio 100% MPF.....	42
Fig. 6-2 Luminance simulation results of MPF case with different curvatures at the backlight thickness of (a) 10 mm, (b) 12 mm, (c) 14 mm, and (d) 16 mm.	45
Fig. 6-3 Initial curvature distribution design of Patterned-MPF at the backlight thickness of 10 mm, 12 mm, 14 mm, and 16 mm.	46
Fig. 6-4 Luminance simulation results of MPF case with designed Patterned-MPF at the backlight thickness of (a) 10 mm, (b) 12 mm, (c) 14 mm, and (d) 16 mm.	47
Fig. 6-5 Optimized curvature distribution design of Patterned-MPF at the backlight thickness of 10 mm, 12 mm, 14 mm, and 16 mm.	47
Fig. 6-6 Relationship between relative output luminance of MPF case with optimized Patterned-MPF and the backlight thickness, where the relative average luminance is normalized to the conventional backlight system (6875 nits).	49
Fig. 7-1 Concave-quadrangular pyramid structure of 2-D MPF.....	53

List of Tables

Table 3-1 Specification of demonstrated backlight system.....	23
Table 5-1 Relative normal brightness and luminance viewing angle.....	39
Table 5-2 Relative output light efficiency.....	40
Table 6-1 Summary of lamp-Mura contrasts in MPF case with initial and optimized Patterned-MPFs.	48
Table 7-1 Comparison of experimental results between the conventional backlight, MPF case, and MPF-Plate case.	52



Chapter 1

Introduction

Liquid-crystal display TVs (LCD-TVs) are popular in recent years because of the advantages, such as high definition, low power consumption, and light weight. In order to produce a bright image from large-size LCD-TVs, direct-emitting backlight systems are mandatory to provide a sufficiently bright and uniform light source. The direct-emitting backlight system consists of optical films, lamps, reflectors and mechanisms, and it has a high cost ratio of whole LCD. Beside, a non-uniform luminance pattern called lamp-Mura is still an issue in direct-emitting backlight systems. The lamp-Mura will cause low quality display images. Therefore, in this thesis, a novel optical film is proposed and designed to suppress the lamp-Mura and reduce the backlight cost.

1.1 Liquid crystal displays (LCDs)

Liquid crystal (LC) is an electro-optic shutter which modulates the transmission of incident light. The configuration of the LC panel module is comprised of glass substrates, LC layers, transparent electrodes, thin film transistors (TFTs), color filters, and polarizers^[1], as shown in Fig.1-1. The LC layer is placed between transparent electrodes (e.g. indium tin oxide, ITO) and driven by a TFT to modulate the light transmission in each pixel of the LCD. The color filter array with three primary colors (red, green, and blue) is fabricated on top glass substrates to produce full color images. The backlight system is placed behind the LC panel to provide a uniform light source for the LCD because the LC is a light switch and cannot emit

light.

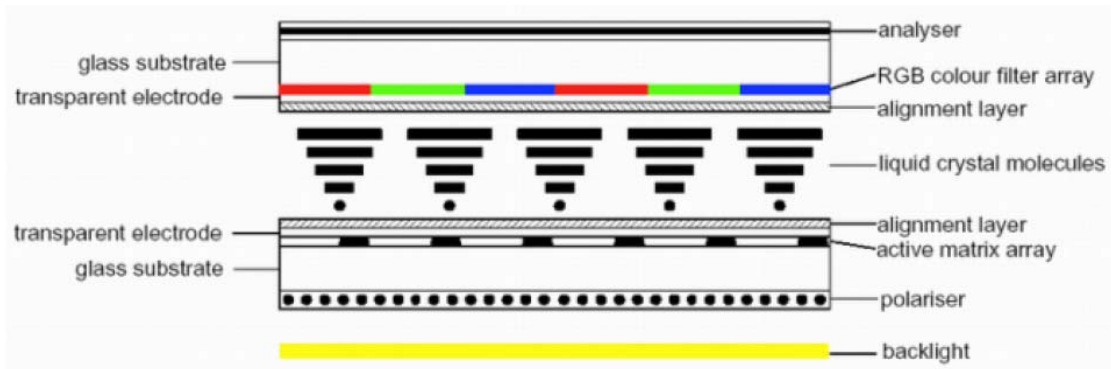


Fig. 1-1 Schematic of a liquid crystal display.

In general, the backlight system can be classified into two types depending on the position of light source (e.g. cold cathode fluorescent lamp (CCFL)) in the LCD. The light source is usually the cold cathode fluorescent lamp (CCFL) or the light emitting diode (LED). The light source at the edge of and directly behind the LCD is called side-emitting and direct-emitting backlights, respectively. A side-emitting backlight is typically used in small and middle-sized LCD because of its small form factor and lower power consumption. However, large-sized LCDs, such as LCD-TVs, have the large display area, thus an increased light source is needed to achieve the specified brightness. Because side-emitting backlight has the limitation of increasing light source, direct-emitting backlight applied to large-sized LCDs is mandatory.

1.2 Direct-emitting backlight systems

A conventional direct-emitting backlight system consists of a diffusive plate, optical films and lamps, as shown in Fig. 1-2. The lamps as a light source are arranged parallel to a LC panel. A diffusive plate with diffusive particles, e.g. PMMA particles, inside the substrate is laid at a distance from the light source. When light is emitted from the light source, it is diffused by the diffusive plate and reflected by the reflector. Then, a bottom diffusive sheet

with adjusted scattering ability is applied to obtain a more uniform light distribution. Then, a prism sheet, which is so-called brightness enhancement film (BEF)^[2], is used to redirect the light from a large inclined angle to the normal direction, thus brightness can be enhanced in the normal viewing direction. Finally, a top diffusive sheet, placed on the top of the backlight system, is applied to protect the micro-structure of the prism sheet and to reduce Moiré patterns^[3].

The backlight system, which includes many components, is high cost in the LCD. The backlight cost ratios of the LCD are 23% using a side-emitting backlight and more than 37% using a direct-emitting backlight, as shown in Fig. 1-3. As the size of the LCD increases, the backlight cost ratio will increase up to 40%^[4]. Therefore, reducing backlight component count and maintaining the quality of backlight system remain a challenge.

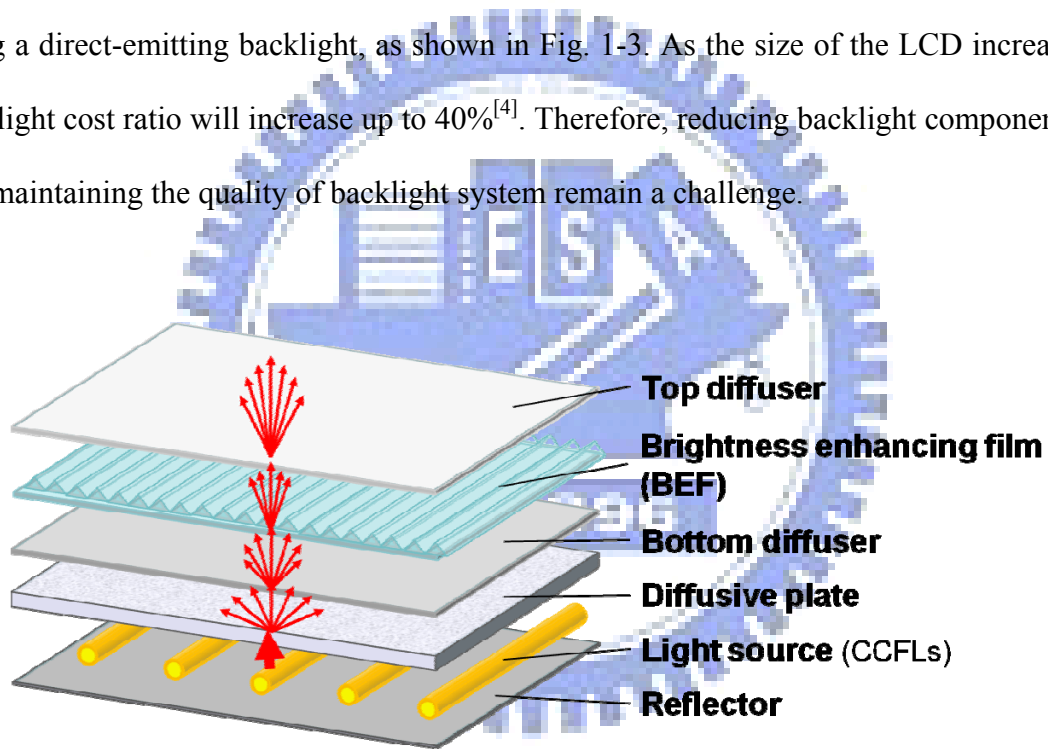


Fig. 1-2 Schematic configuration of a direct-emitting backlight system.

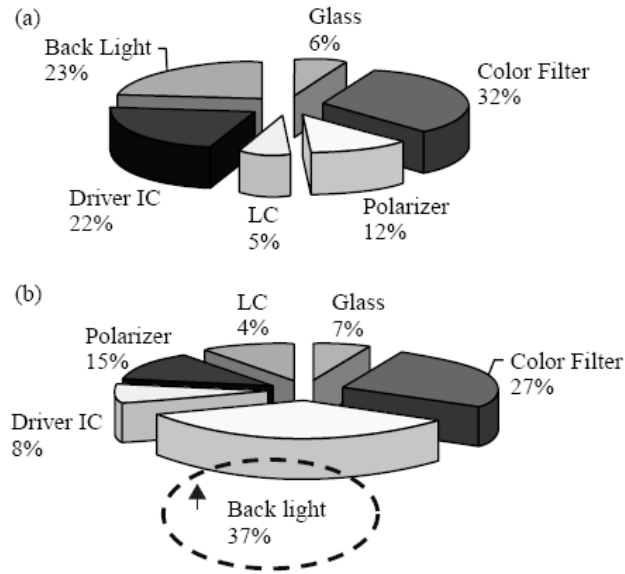


Fig. 1-3 The ratio of the backlight cost of (a) 15-inch side-emitting and (b) 30-inch direct-emitting backlight in the LCD^[4].

1.3 Lamp-Mura issue

Compared with the side-emitting backlight, the direct-emitting backlight has issues, such as higher power consumption, greater thickness, higher cost and lamp-Mura defect^[5]. Lamp-Mura is a non-uniform periodic luminance pattern which exists in direct-emitting backlight systems. A lamp-Mura example of a direct-emitting backlight is shown in Fig. 1-4. Lamp-Mura is caused by strong brightness lamps and poor diffusive ability optical films.



Fig. 1-4 Lamp-Mura defect of a 32-inch direct-emitting backlight system captured by a charge-coupled device (CCD).

Currently, there are straightforward methods to improve lamp-Mura that have been summarized by Schiavoni^[6]:

- Increasing lamps or decreasing the gap between lamps can improve lamp-Mura. However, power consumption and cost are increased.
- Large distance from lamps to diffusive plates improves lamp-Mura. However, greater thickness is not a current trend in the display market.
- Plurality of diffusive films in the stack suppresses lamp-Mura. For example, diffusive plates and diffusive sheets are usually applied to increase uniformity of backlight systems. However, increased diffusive films, higher cost.

The methods mentioned above can improve lamp-Mura, but cost and greater thickness are not helpful to backlight systems. Other researches are also proposed to improve lamp-Mura. Seon et al., used a prism shape reflector at the center between two lamps to control reflected light^[7]. The results show lamp-Mura can be improved even when number of lamps is reduced. Schiavoni et al., also proposed a novel glass diffuser plate with variational coating thickness and scattering particle density to improve lamp-Mura^[6]. In addition, Kang et al., proposed a diffusion plate with transfectors^[8]. However, these prior methods have extra components and cost, and decreased average brightness.

1.4 Motivation and objectives

For producing a bright display image in large-size LCDs, direct-emitting backlight systems are used to provide a sufficiently bright and uniform light source. Since the backlight system consists of optical films, reflectors and lamps, high cost is an issue of backlight systems. Besides, lamp-Mura, an issue in the direct-emitting backlight system, will degrade the display image quality of LCDs. Several general solutions have been proposed, but they caused increased optical films and higher cost. In order to suppress lamp-Mura without increasing the cost of the backlight system, one way is to study optical films, such as diffusive films and micro-structure films, how to suppress lamp-Mura effectively.

In this thesis, a multi-performance film (MPF) was designed to suppress lamp-Mura in direct-emitting backlight systems^[9]. We expect that the lamp-Mura contrast of using MPFs can smaller than 0.012, where this target value is come from a conventional backlight without lamp-Mura. Moreover, designed micro-structures on the top of MPFs were fabricated by the screen printing process, supported by E vendor^[10]. By using the MPF of optimized concave prism profile, we expect that one or more diffusive films can be eliminated, in addition, the viewing angle and the output light efficiency of backlight systems can be enhanced.

Slim LCD-TVs are a trend in current display market because it can mount on a wall to free up more space. However, the lamp-Mura will become more serious when the backlight thickness is decreased. For a slim and low-cost backlight system, the MPF has a limited capability to suppress lamp-Mura because of the uniform micro-structures of MPFs. The lamp-Mura is caused by a non-uniform light distribution, which the luminance is varied in different spatial positions. If the micro-structure profile of MPF can be adjusted according to the spatial light distribution, an improved uniformity of light distribution will be achieved. Therefore, a patterned-MPF, which has different micro-structure shapes depending on the distance from lamps, was proposed for reducing the backlight thickness.

1.5 Organization of this Thesis

The thesis is organized as follows: The principles of backlight systems are presented in **Chapter 2**. In **Chapter 3**, the fabrication of the MPF is introduced, and the major instruments for characterizing backlight systems are also described. The design concepts and simulation results of MPFs are presented in **Chapter 4**. The experimental results are presented in **Chapter 5**. In **Chapter 6**, the design of Patterned-MPFs and simulation results are described. Finally, conclusions of this thesis and recommendations for the future work are presented in **Chapter 7**.



Chapter 2

Principles of backlight system

For designing and analyzing backlight unit, several optical principles, such as Snell's law, Fresnel's law, and bidirectional scattering distribution function (BSDF), were described in this chapter. The ray-tracing method simplifies light propagation behavior as a ray. However, scatter properties of diffusive films in backlight systems are difficult to describe by using the ray-tracing. Accordingly, BSDF was used to characterize diffusive films, and BSDF characteristics were then measured. The measured BSDF data were imported to ray-tracing software, LightTools^[11], for building diffusive film models. Moreover, work principle and issues of brightness enhancement films (BEFs) were also presented.

2.1 Ray-tracing method

Ray-tracing method is based on the geometrical optics, Fresnel's Law and other principles. Geometrical optics, so-called ray optics, is the subject which describes light propagation behavior as a ray. If light waves are radiated from a point source in a vacuum, it is apparent that at a given instant each wave front is spherical. The curvature of the wave front is decreased as the wave front travels away from the point source. At a sufficient distance from the source, the radius of the wave front may be regarded as infinite. Such a wave front is called a plane wave. If we trace the path of a hypothetical point on the surface of a wave front as it moves through space, the point progress is like a straight line. The path of the point is thus called a ray of light^[12]. Such a light ray is an extremely convenient fiction, of great utility

in understanding and analyzing the action of optical systems. Therefore, some optical softwares, such as LightToolsTM, TraceProTM, et al., apply the geometrical optics to build optical modules for a simulated environment.

Law of refraction (Snell's law)

A light ray incident on a boundary surface results in refracted and reflected rays. The incident ray, the normal direction of the sample surface, the reflected ray and the refracted ray are on a common plane which called the plane of incidence. In the plane of incidence, the angle, θ_i , between the surface normal and the refracted ray (the refraction angle) satisfies the following equation^[13],

$$n_i \sin \theta_i = n_t \sin \theta_t, \quad (1)$$

where θ_i is the angle between the normal direction of surface and the incident ray (the incidence angle), n_i and n_t are the refractive indices of the incident and transmitting mediums, respectively. This equation is the law of refraction, also known as Snell's law.

Law of reflection

All of the light incident upon a boundary surface is not transmitted through the surface; some portion is reflected back into the incident medium. The angle, θ_r , between the normal direction of surface and the reflected ray (the reflection angle) is equal to the incidence angle. Thus, for reflection, Snell's law takes on the form^[14]:

$$\theta_i = \theta_r, \quad (2)$$

which is the so-called law of reflection.

Total internal reflection

According to Snell's law in the case of internal reflection ($n_i > n_t$), the critical angle θ_c is that special value of θ_i for which $\theta_t = 90^\circ$. The formula of the critical angle θ_c is as follows^[15]:

$$\theta_c = \sin^{-1}\left(\frac{n_t}{n_i}\right) \quad (3)$$

When incident angles θ_i greater than or equal to θ_c , all the incoming energy is reflected back into the incident medium, this process is known as total internal reflection.

Fresnel's law

Fresnel's law describes the transmission and reflection of light at the interface of two different materials. According to electromagnetic theory, light is a kind of electromagnetic wave which includes an electric field \mathbf{E} and a magnetic field \mathbf{B} , and satisfies Maxwell's equations. Assume a monochromatic plane wave is incident on the boundary surface separating two isotropic media, then, Fresnel equations including the amplitude reflection coefficient r and the amplitude transmission coefficient t of the electric field are as follows^[16]:

$$r_{\perp} \equiv \left(\frac{E_{or}}{E_{oi}} \right)_{\perp} = \frac{n_i \cos \theta_i - n_t \cos \theta_t}{n_i \cos \theta_i + n_t \cos \theta_t} \quad (4)$$

$$t_{\perp} \equiv \left(\frac{E_{ot}}{E_{oi}} \right)_{\perp} = \frac{2n_i \cos \theta_i}{n_i \cos \theta_i + n_t \cos \theta_t} \quad (5)$$

$$r_{\parallel} \equiv \left(\frac{E_{or}}{E_{oi}} \right)_{\parallel} = \frac{n_t \cos \theta_i - n_i \cos \theta_t}{n_i \cos \theta_i + n_t \cos \theta_t} \quad (6)$$

$$t_{\parallel} \equiv \left(\frac{E_{ot}}{E_{oi}} \right)_{\parallel} = \frac{2n_i \cos \theta_i}{n_i \cos \theta_i + n_t \cos \theta_t} \quad (7)$$

where suffixes \perp and \parallel means the direction of electric field E perpendicular and parallel to the plane of incidence, respectively.

According to the definition of irradiance^[17], the reflection R and transmission T of light energy is proportional to r^2 and t^2 . For a natural light which has random polarizations, the transmission and reflection are as follows:

$$R = \frac{R_{\perp} + R_{\parallel}}{2} = \frac{r_{\perp}^2 + r_{\parallel}^2}{2} \quad (8)$$

$$T = \frac{T_{\perp} + T_{\parallel}}{2} = \frac{t_{\perp}^2 + t_{\parallel}^2}{2} \quad (9)$$

According to the laws of refraction and reflection, the trace of ray propagating is found. Moreover, the transmission and reflection of a ray at an interface can be obtained by Fresnel's law, and finally the light energy of a ray on a defined receiver can be calculated. Therefore, ray-tracing is suitable to assist our backlight design processes.

2.2 Lamp-Mura contrast

To analyze lamp-Mura, "lamp-Mura contrast," an index related to the spatial sensitivity of the human eye in different spatial frequencies, is used to evaluate the degree of lamp-Mura^{[6],[18]}. The lamp-Mura contrast is defined as follows:

$$\text{Lamp-Mura contrast} = \frac{L_{\max} - L_{\min}}{L_{\max} + L_{\min}} \quad (10)$$

where L_{\max} and L_{\min} are the maximum and minimum luminance of the lamp-Mura pattern, respectively, as shown in Fig. 2-1. The lower the lamp-Mura contrast, the less lamp-Mura is observed.

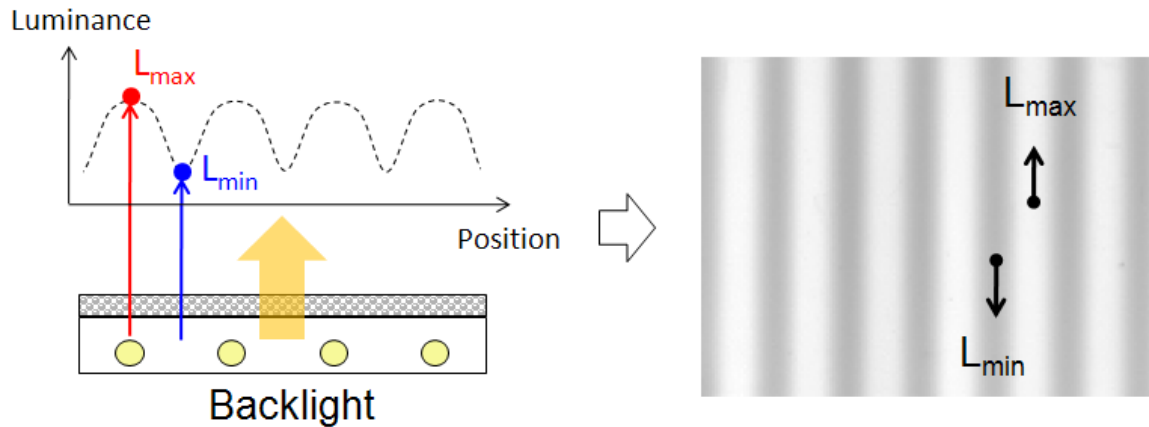


Fig. 2-1 Diagram of lamp-Mura.

2.3 Bidirectional scatter distribution function (BSDF)

The bidirectional scatter distribution function (BSDF) is commonly used to describe scattered light distributions. The terms BRDF, BTDF, and BVDF, used for reflective, transmissive, and volume samples, are merely subsets of the more generic BSDF. In this thesis, BTDF and BRDF were adopted to characterize diffusive films and reflectors.

The defining geometry of BTDF and BRDF is shown in Fig. 2-2 where the subscripts i , t and r are denoted for incident, reflected and transmitted quantities, respectively. The notation θ is the azimuthal angle between light direction and the normal direction of sample surface, and ϕ is the polar angle on the sample surface.

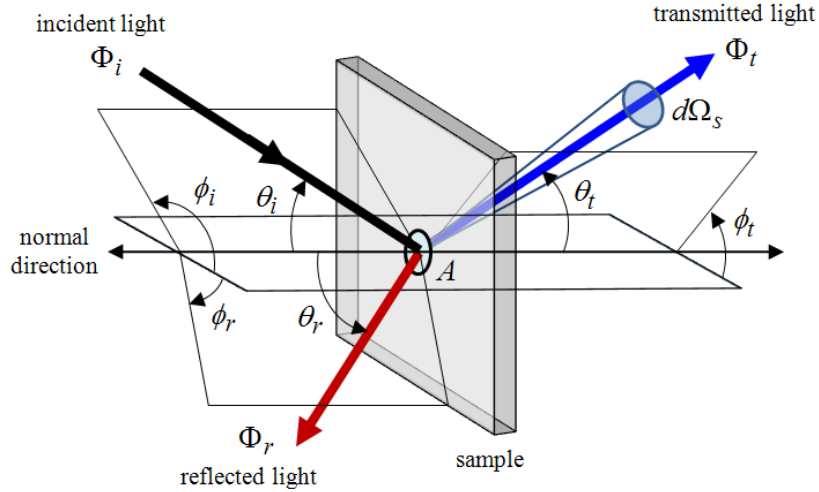


Fig. 2-2 Schematic of BSDF.

If a collimated beam is illuminated on the sample with an area A , the BTDF and BRDF are then defined as scattered luminance (dL_t and dL_r) divided by incident illuminance (E_i) as follows

$$BTDF(\theta_i, \phi_i, \theta_t, \phi_t) \equiv \frac{dL_t(\theta_i, \phi_i, \theta_t, \phi_t)}{E_i(\theta_i, \phi_i)} \quad (11)$$

$$BRDF(\theta_i, \phi_i, \theta_r, \phi_r) \equiv \frac{dL_r(\theta_i, \phi_i, \theta_r, \phi_r)}{E_i(\theta_i, \phi_i)} \quad (12)$$

The scattered luminance is light flux scattered through a solid angle $d\Omega_s$ per unit illuminated surface area per unit projected solid angle. The projected solid angle is the solid angle ($d\Omega_s$) multiplied by $\cos \theta_s$. The BSDF is then defined to include BTDF and BRDF, and becomes

$$BSDF \equiv \frac{dL_s}{E_i} \cong \frac{d\Phi_s / d\Omega_s}{\Phi_i \cos \theta_s} \quad (13)$$

where dL_s includes dL_t and dL_r , θ_s includes θ_t and θ_r , Φ_i and $d\Phi_s$ are the incident and scattered luminance flux. This equation is appropriate for all incidence angles and all scattered angles. The term $d\Phi_s / \Phi_i$ of BSDF means the transmittance of scattered

light in (θ_s, ϕ_s) direction, which it can be obtained by measuring the incident illuminance and the scattered luminance. Thus, BSDF can generate scatter specifications of samples that enable optical designers, manufacturers and users to communicate and check requirements.

In this thesis, the BTDF of diffusive films was measured by our designed BTDF measurement device, and the BRDF of reflectors was measured by a conoscopic system in reflective mode. To start our design, the measured BTDF and BRDF data was imported to optical software, LightTools, to build optical models corresponding with backlight components.

2.4 Principle of brightness enhancement film (BEF)

The function of brightness enhancement film (BEF) is to enhance the brightness of backlight systems. A conventional BEF is composed of a bottom substrate and micro-prism structures, where the shape of the prism is commonly triangular. In this thesis, the used BEF was supported by E vendor, where the materials of the prism and substrate are PET and PMMA, respectively, and the prism vertex angle is 90° .

An example of BEF to explain its working principle is shown in Fig. 2-3. When a Lambertian light (a uniform angular luminance distribution) was imported to BEF, the prism structure causes light refraction (c, Fig. 2-3). Additionally, the effect of total internal reflection (TIR) occurs continuously till the incident angle is larger than the specific critical angle (b, Fig. 2-3). Therefore, all rays are gathered within a 35-degree cone in the normal direction.

Because output luminance cone is limited by BEF, the output luminance viewing angle is decreased comparing to the input one, as shown in Fig. 2-4. The luminance viewing angle is defined as full width of half maximum (FWHM) luminance. Thus, the low luminance viewing angle results dark display images observed from a large viewing angle. These display images

is obviously darker than that observed from the normal direction. As a result, BEF enhanced the normal brightness but decreased the luminance viewing angle; it was a tradeoff between brightness and luminance viewing angle.

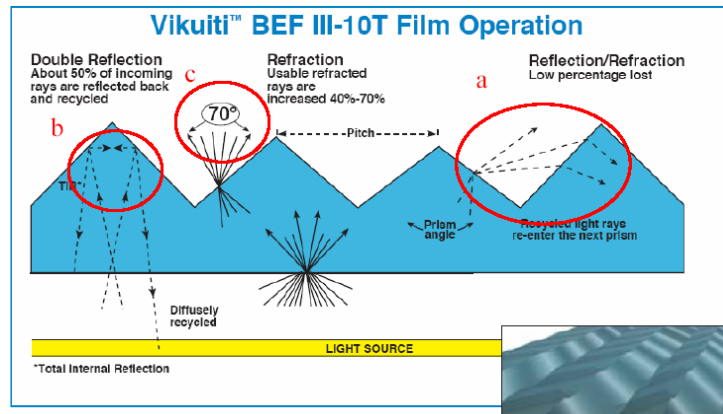


Fig. 2-3 Diagram of BEF working principle^[19]

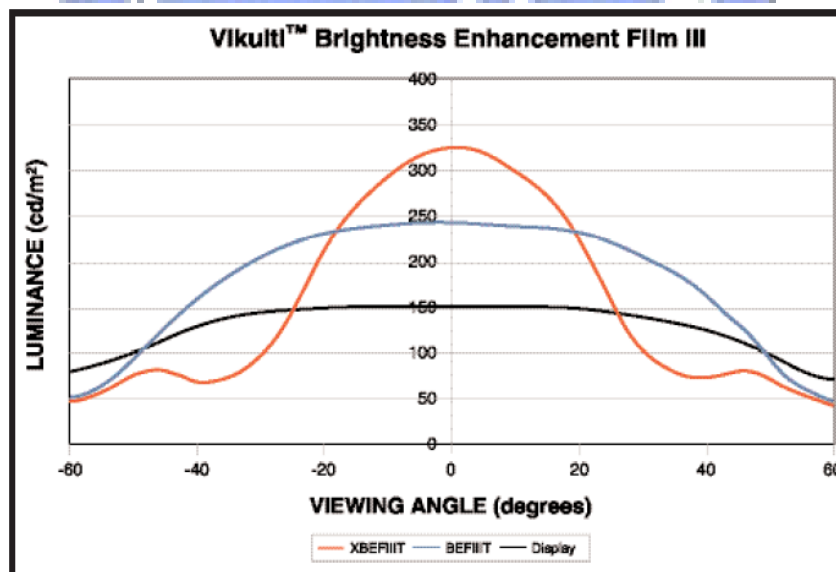


Fig. 2-4 Diagram of the angular distribution using BEF III, where the black line is without any BEF; the blue line added a BEF; and the red line placed two BEFs crossed at 90°^[19].

For BEF, the uniformity of input light distribution would affect that of the output. If a non-uniform light distribution was input to a BEF, the output would also non-uniform. For example, a test which captured output images from a backlight system with and without a BEF is shown in Fig. 2-5 (c). For the backlight system only had a diffusive plate (Fig. 2-5 (a)), lamp-Mura is clearly observed. The luminance above lamps is higher than that between two lamps. If a BEF is placed on the diffusive plate (Fig. 2-5 (b)), lamp-Mura still exists but the positions of relatively maximum and minimum luminance are altered. This phenomenon can be explained by using ray-tracing as shown in Fig. 2-6. When normal incident light inputs to a BEF, it is blocked by the prism structure because of the total internal reflection (TIR), and the luminance above lamps is decreased. But oblique incident light can be redirected to enhance the brightness at the normal direction by using a BEF.

As a result, BEF could enhance normal brightness, but it also decreased the luminance viewing angle. Moreover, from the captured image (Fig. 2-5 (c)), we can find that lamp-Mura becomes slighter after adding a BEF, but it still can be observed. In order to resolve these issues, we proposed a multi-performance film (MFP) to replace a conventional BEF and to suppress lamp-Mura.

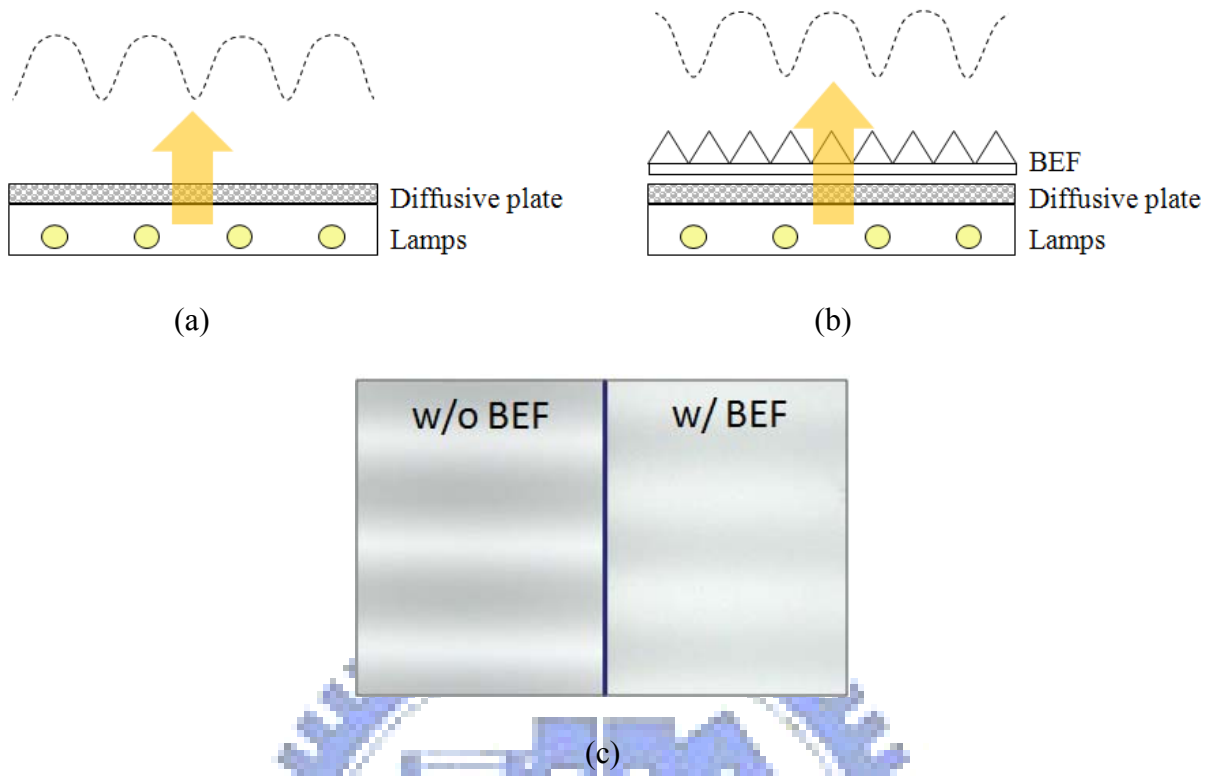


Fig. 2-5 Schematics of the backlight luminance distribution (a) without and (b) with a BEF, and (c) measurement results.

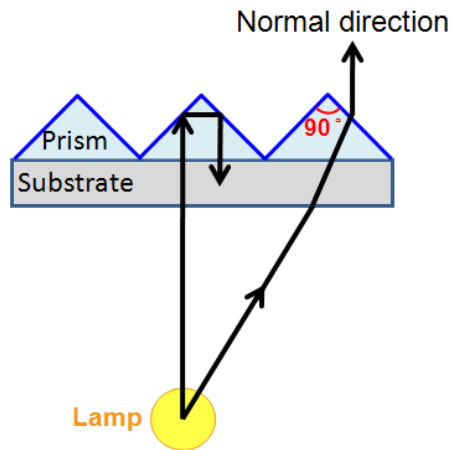


Fig. 2-6 Schematic of ray-tracing in a BEF.

2.5 Summary

Ray-tracing method was used to design backlight system in this thesis. Law of reflection and reflection, TIR, and Fresnel's law, can describe the propagation trajectory and the carried power of light. Thus, the optical software, LightTools, based on the ray-tracing method was used to simulate a backlight system. We then created optical film models which can be characterized by BSDFs of optical films. In order to evaluate the degree of lamp-Mura, the lamp-Mura contrast was defined. The lower the lamp-Mura contrast, less lamp-Mura can be observed. Besides, we found that BEF enhanced brightness but did not improve lamp-Mura well, because the triangular prism structure of BEF had no scattering ability. Therefore, an optical film which integrated brightness-enhancement and light-scattering functions will be designed to suppress lamp-Mura.



Chapter 3

Design and simulation of MPF

A multi-performance film (MPF) with concave-prism structures was designed to replace a conventional brightness enhancement film (BEF) and to improve the optical performance of backlight systems. For saving optical films and suppressing lamp-Mura, two backlight structures with MPFs were designed. By using the simulation software, LightTools, simulation models of real objects were built. Additionally, the curvatures in MPF and MPF-Plate case were optimized to suppress lamp-Mura.

3.1 Design of MPF

The multi-performance film (MPF) was modified from a conventional BEF. As mentioned in Chapter 2, if a non-uniform light distribution was input to a conventional BEF, the oblique incident light could be redirected to enhance brightness at normal direction. But normal incident light was blocked by the prism structure according to the total internal reflection (TIR), and the luminance above lamps was decreased. Additionally, the lamp-Mura still existed after adding the BEF. If the relative maximum and minimum luminance after a BEF can be balanced, lamp-Mura will be improved. Therefore, a multi-performance film (MPF) with concave-prism structures was proposed to replace the original BEF for improving lamp-Mura, as shown in Fig. 3-1. A parabolic curve was proposed as the profile for concave-prism structures in this research. The formula of the parabola is:

$$z = z_0 + \frac{C}{2} x^2, \quad (14)$$

where z is the vertical distance from the substrate, x is the horizontal position, C is curvature of the parabola and z_0 is the vertical shift distance to meet designed prism width.

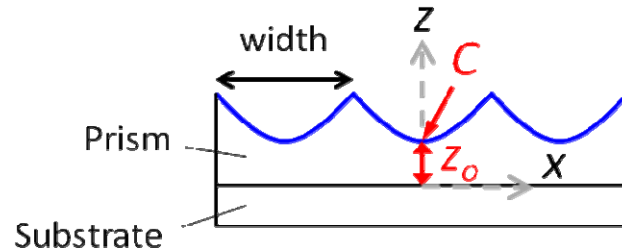


Fig. 3-1 Schematic of MPFs.

Ray-tracing results were used to describe light propagated through BEF and MPF, as shown in Fig. 3-2. When incident light was input into MPF, concave-prism structures of MPF caused a light divergence which is similar to the scattering property of diffusers. The oblique incident light also was redirected to normal direction to enhance brightness. Therefore, MPF simultaneously included the scattering function as a diffuser and the brightness enhancement function as a conventional BEF. Moreover, the normal incident light partially passed through MPF to enhance normal brightness, and the luminance at the center between two lamps was still remained as a BEF. Thus, we conclude the luminance difference between the maximum and the minimum can be reduced by MPF; on the other hand, the uniformity can be increased, as shown in Fig. 3-3.

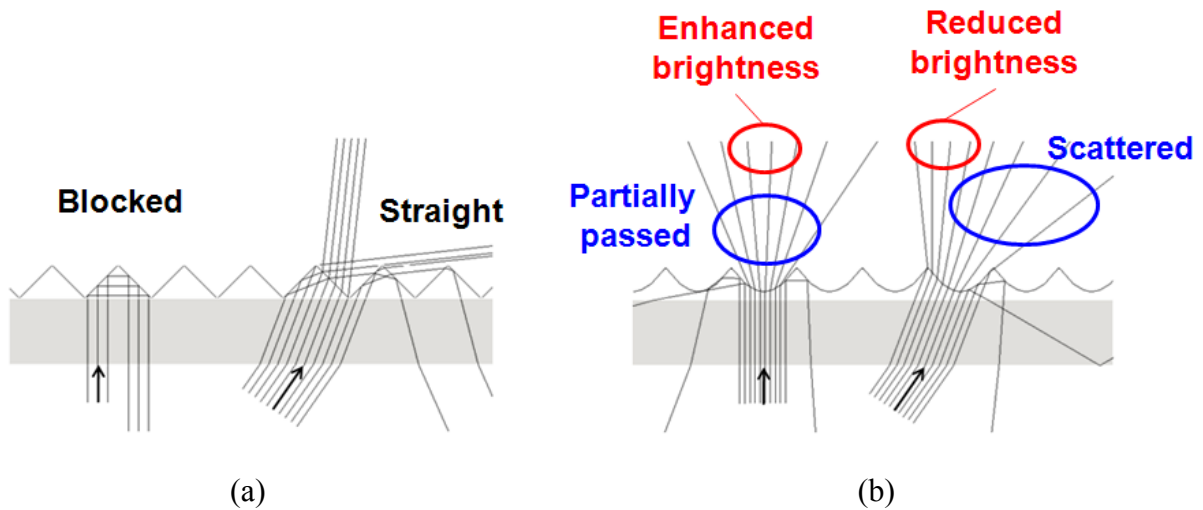


Fig. 3-2 Ray-tracing diagrams of (a) conventional BEF and (b) MPF.

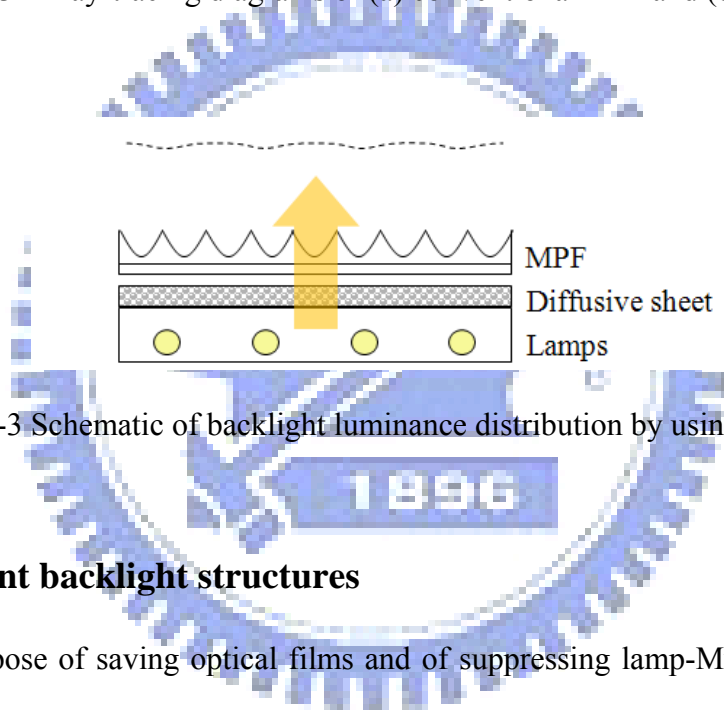


Fig. 3-3 Schematic of backlight luminance distribution by using a MPF.

3.2 Experiment backlight structures

For the propose of saving optical films and of suppressing lamp-Mura, two experiment backlight structures, MPF and MPF-Plate case, were designed to compare with the conventional backlight structure, as shown in Fig. 3-4. For designed MPF case, a MPF and an acrylic transparent plate replaced the BEF III and the highly efficient diffusive plate (HEDP) in the conventional backlight system, respectively. The advantage of MPF case is that the transparent plate has lower cost than the diffusive plate. However, several interfaces of optical films resulted in Fresnel loss to reduce the transmission light efficiency. Therefore, the MPF-Plate, which integrated the MPF and the diffusive plate, was designed to enhance the

output light efficiency. In the following simulation, curvatures of MPFs will be optimized for suppressing lamp-Mura.

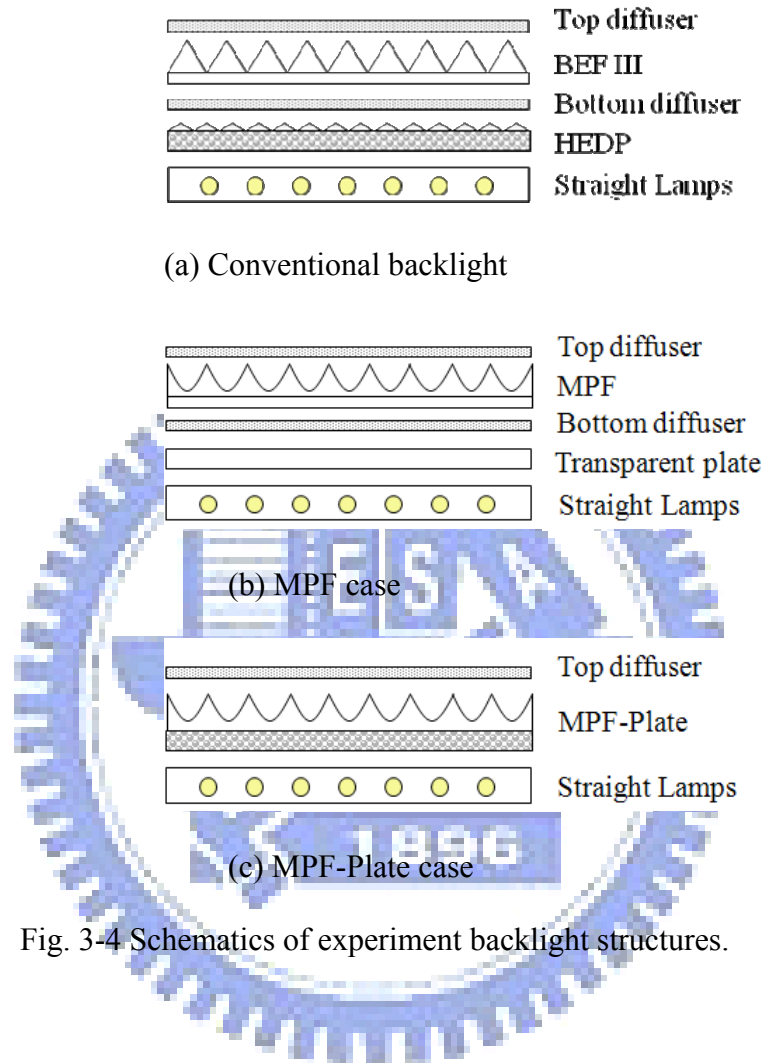


Fig. 3-4 Schematics of experiment backlight structures.

3.3 Specification of demonstrated backlight system

For optimizing MPF in the backlight structure, a common LCD-TV backlight system was adopted to be our design platform, whose specification is shown in Table 3-1. The backlight system had 32-inch display area and 12 lamps on the bottom as shown in Fig. 3-5, and the horizontal and vertical directions were also defined. The specification then was imported to the simulation software to model real objects.

Table 3-1 Specification of demonstrated backlight system.

Item	Value
Backlight size (Inch)	32
Backlight thickness* (mm)	20
Number of lamps	12
Lamp pitch** (mm)	33
Lamp height*** (mm)	3
Lamp diameter (mm)	3
Input power (per lamp) (W)	5
Brightness (per lamp) (Nit)	20000

* The distance from the reflector to optical films

** The distance between two lamps

*** The distance from the reflector to the lamp

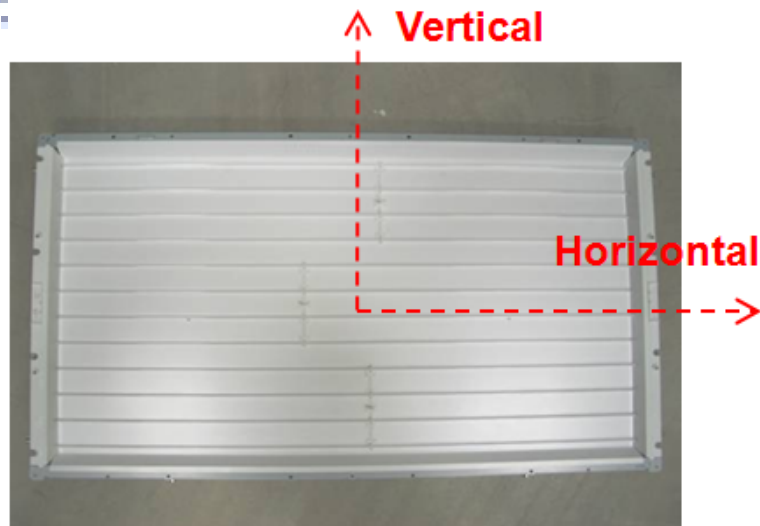
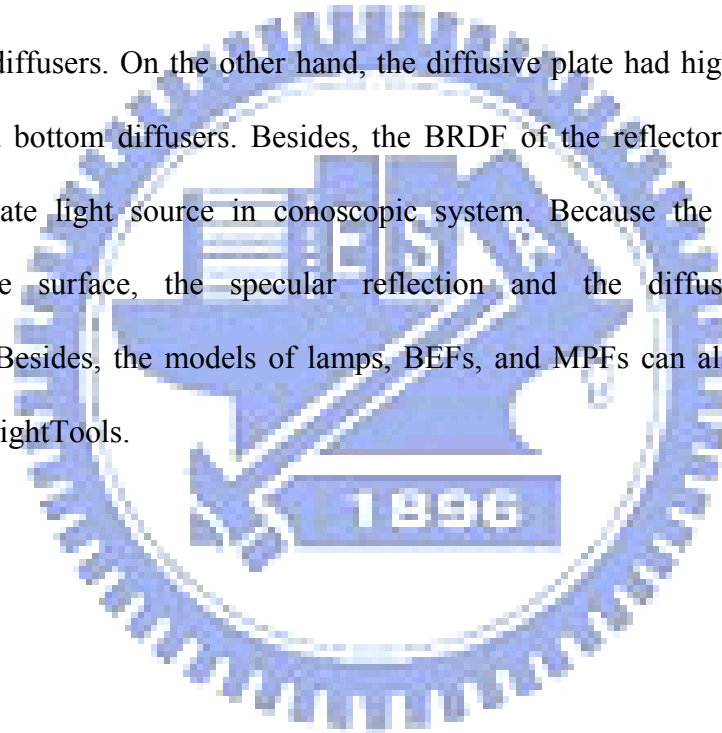


Fig. 3-5 Demonstration of a 32-inch backlight system.

3.4 Simulation models

The simulation software, LightTools, was adopted to design the MPF in this thesis. LightTools can model real objects and it follows the ray-tracing method in simulation. The bidirectional transmissive/reflective distribution function (BTDF/BRDF) of diffusive films and reflectors are shown in Fig. 3-6. A BTDF measurement device and a conoscopic system, which will be introduced in Chapter 4, were used to measure these BTDFs and BRDFs. The BTDFs of top and bottom diffuser were similar and had transmission light peaks at incident angles 0° to 20° . The BTDF of diffusive plate was smoother and wider compared with that of top and bottom diffusers. On the other hand, the diffusive plate had higher scattering ability than the top and bottom diffusers. Besides, the BRDF of the reflector was measured with reflective collimate light source in conoscopic system. Because the reflector had white particles on the surface, the specular reflection and the diffusion were occurred simultaneously. Besides, the models of lamps, BEFs, and MPFs can also be created by the build-in tool in LightTools.



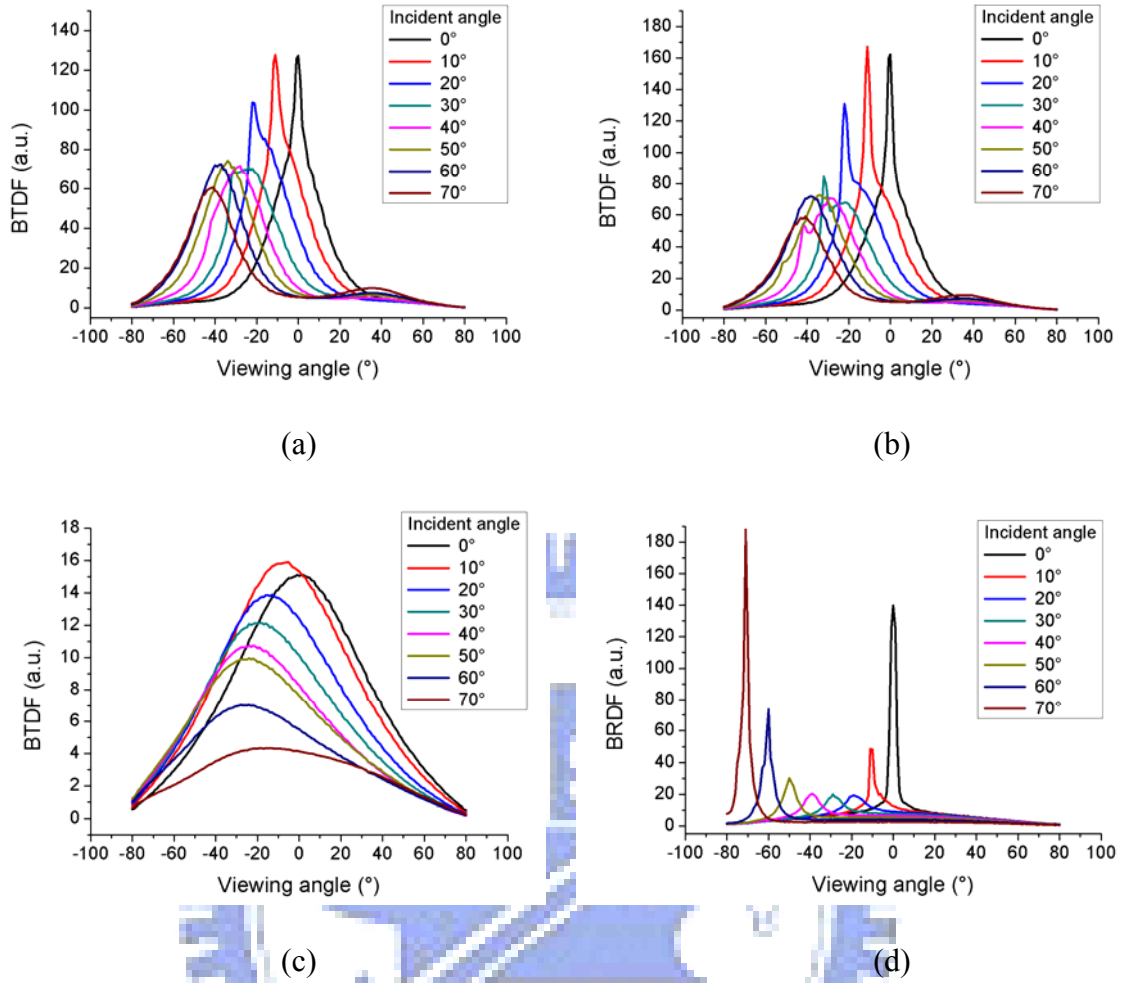


Fig. 3-6 Measured BTDFs of the (a) top diffuser, (b) bottom diffuser, and (c) diffusive plate, and BRDF of the (d) reflector.

3.5 Simulation results

To suppress lamp-Mura, the curvatures of MPF and MPF-Plate case will be optimized according to the lamp-Mura contrast result. The lamp-Mura contrast defined in Section 2.2 was calculated according to the spatially luminance distribution form backlight systems. The spatially normal luminance distributions were determined by luminance data of 33 points between two lamps at the backlight system center, as shown in Fig. 3-7. From the figure, the 0 and the 1 pitch are positions above lamps, and the 0.5 pitch is the center position. Compared with MPF case included a MPF, MPF case with a conventional BEF had a higher luminance

at the center position than above lamps, as shown in Fig. 3-7 (a). Additionally, MPF case enhanced the luminance above lamps for a more uniform light distribution. In order to evaluate whether the light distribution is uniform enough for suppressing lamp-Mura, the lamp-Mura contrasts of MPF and MPF-Plate case will be calculated.

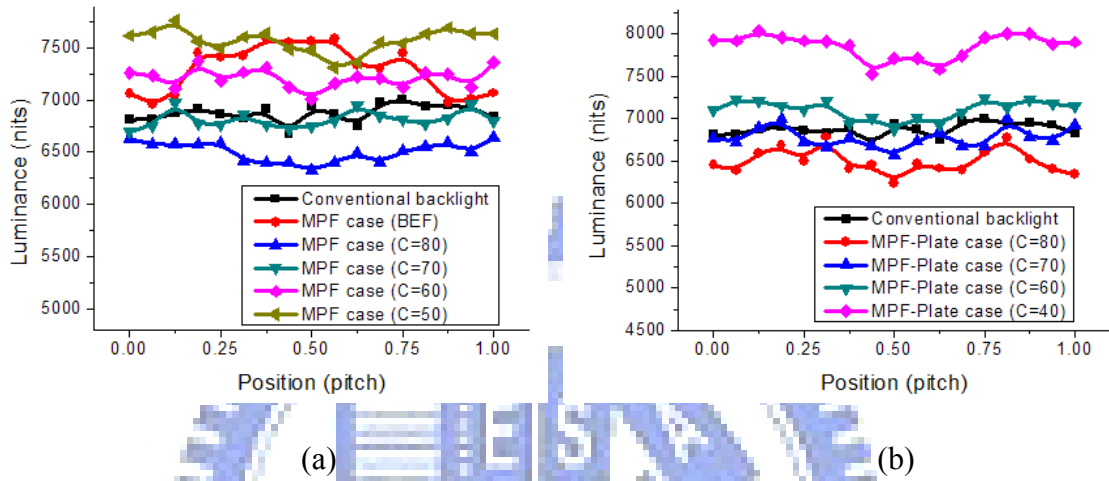


Fig. 3-7 Luminance distributions of (a) MPF case and (b) MPF-Plate case, where C is curvature.

3.5.1 Lamp-Mura contrast and optimized curvature

Lamp-Mura contrasts of different MPF curvatures in MPF and MPF-Plate case are shown in Fig. 3-8. For MPF case, the optimized MPF curvature range from 57 to 81 mm^{-1} had smaller lamp-Mura contrast than the conventional backlight. For MPF-Plate case, the optimized MPF curvature was about 60 mm^{-1} the closest to the conventional backlight. Because the conventional backlight had invisible lamp-Mura, thus, we conclude MPF and MPF-Plate case with optimized curvature also can suppress lamp-Mura.

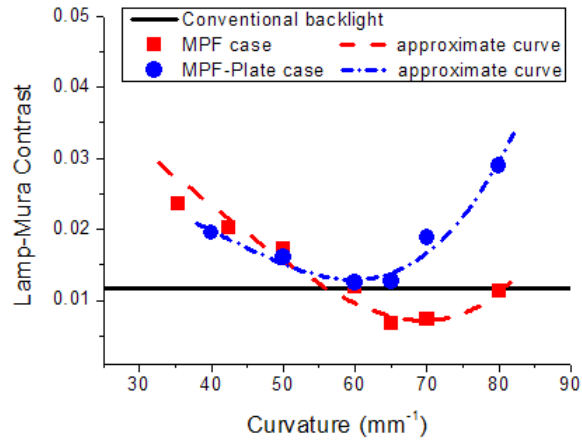


Fig. 3-8 Lamp-Mura contrast of MPF and MPF-Plate case.

3.5.2 Average luminance

The average luminance between two lamps was also obtained, as shown in Fig. 3-9. The luminance of MPF case decreased when the MPF curvature increased over 70 mm⁻¹. This situation was similar to MPF-Plate case with the threshold MPF curvature of 67 mm⁻¹. Additionally, the luminance of MPF-Plate case in curvature range, 40~75 mm⁻¹, is lower than that of MPF case. At optimized curvature 60 mm⁻¹, MPF-Plate case yielded 2% decrease in luminance (7243 nits → 7070 nits) compared with MPF case. However, most important is that both cases had higher luminance than the conventional backlight system.

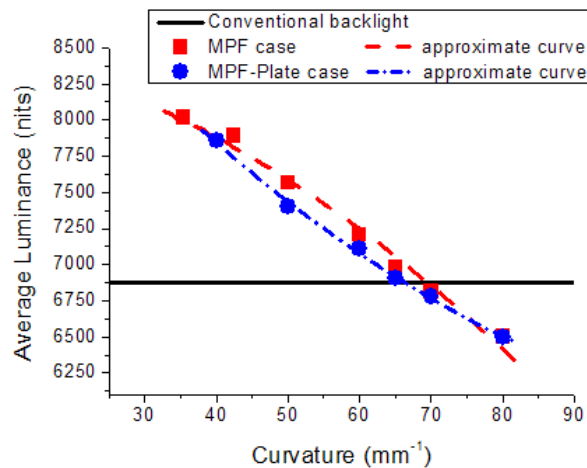
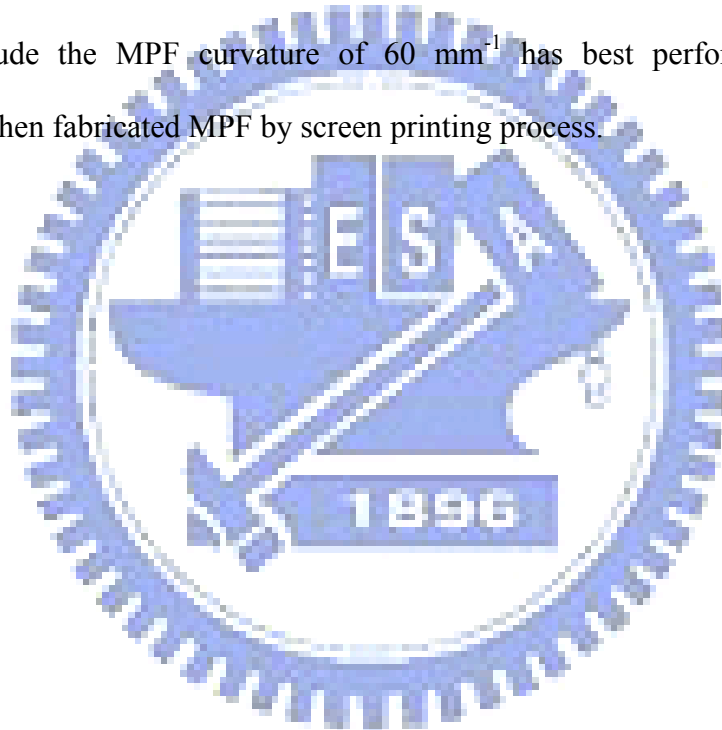


Fig. 3-9 Average luminance of MPF and MPF-Plate case.

3.6 Summary

The concave prism profile of MPF was designed as parabola, and the curvature is the designed parameter. For optimizing the MPF curvature, backlight component models were built to create a simulation environment by LightTools. Additionally, MPF and MPF-Plate case with MPFs were designed to compare with the conventional backlight system. In the simulation, lamp-Mura contrast results were obtained. Then, the optimized curvature of MPF and MPF-Plate case, which had less lamp-Mura contrast as the conventional backlight, was found about 60 mm^{-1} . Moreover, a higher luminance was also obtained at curvature 60 mm^{-1} . Thus, we conclude the MPF curvature of 60 mm^{-1} has best performance to suppress lamp-Mura. We then fabricated MPF by screen printing process.



Chapter 4

Fabrication technologies and measurement instruments

Optical devices with micro-structures, such as prisms, micro-lens and diffractive optical elements, are generally used in micro-electro-mechanical systems (MEMS), display devices and projectors, et al. For devices with feature size of $1\mu\text{m} \sim 1\text{mm}$, photolithography and etching techniques (standard semiconductor processes), diamond machining and excimer laser micro-machining (laser ablation) are applicable^[20]. These methods are complex and are not efficient in fabricating the proposed MPF concave-prism structures. Therefore, an easy and economical fabrication method, screen printing process, supported by E vendor was adopted to fabricate MPF. Moreover, several instruments for measuring MPF profiles and optical performances of designed backlight systems are also introduced in this chapter.

4.1 Screen printing process of MPFs

The concept to fabricate the MPF concave-prism profile is to fill a UV-curable material on a conventional BEF, where this material has the same refractive index to the prism structure. The MPF fabrication schematic by using screen printing process is shown in Fig. 4-1. The dimension of the used BEF is $25\mu\text{m}$ height and $50\mu\text{m}$ width as shown in Fig. 4-2. For controlling the amount of material filled, first, a mask (so-called screen) with a designed aperture ratio distribution was placed on a conventional BEF. Second, the UV-curable

material was dropped on the mask. Third, a squeegee, which is a flexible rubber, pressed and horizontally moved over the mask. Then, the UV-curable material flowed through mask apertures to fill the prism grooves on the BEF. Finally, a filled concave profile was formed after curing the filled material in UV-exposure.

According to the designed aperture ratio of the mask, the amount of filled material could be controlled to make different concave-prism profiles of MPFs. In this thesis, the term “filling ratio (%)” depended on the mask aperture ratio was applied to classify different filling profiles of MPFs.

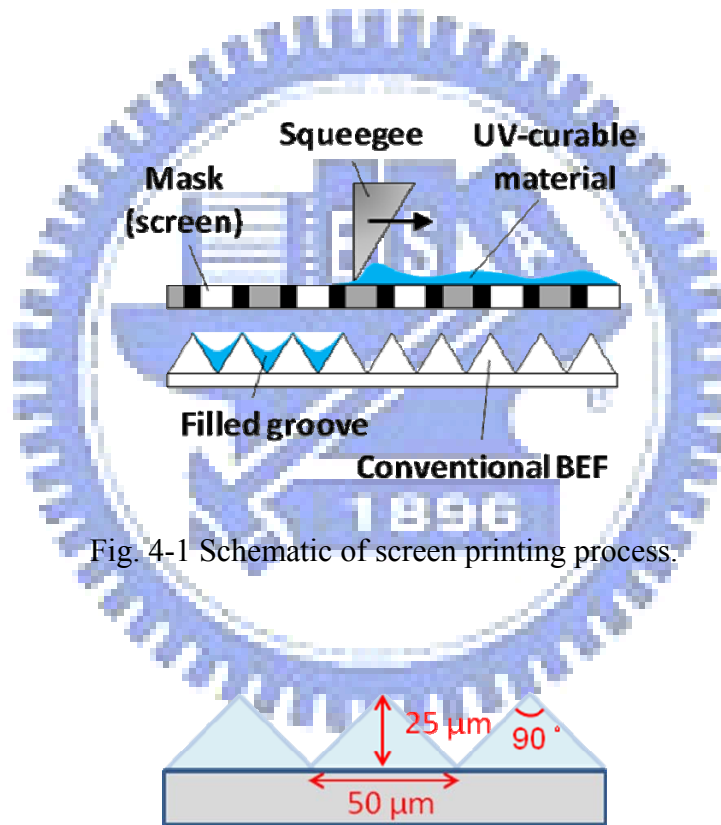


Fig. 4-1 Schematic of screen printing process.

Fig. 4-2 Schematic of used BEF structure.

4.2 Measurement instruments

After the fabrication, fabricated MPF profiles were examined and measured by an optical microscope (OM) and the surface profiler, Alpha-Step IQ^[21], respectively. Then, optical performances of backlight systems were measured using a conoscopic system and a

charge-coupled device (CCD). In order to set up the diffusive plate and diffuser models in our simulation, our designed bidirectional transmittance distribution function (BTDF) measurement device was used to extract scatter properties of diffusive films to import into the simulation software, LightTools™.

4.2.1 Conoscopic system

The conoscopic system applies Fourier transform lens to transfer light beams emitted from the test area to a CCD array. Therefore, the angular properties could be easily measured on the CCD sensor plane. The CCD array consists of various directional CCD sensors to detect brightness, color, and angular distribution of transmissive light. Besides, it has two modes for measuring transmissive or reflective light. In our experiment, the transmissive mode is employed because the backlight system can emit light itself.

The options for testing under illumination are based on the combination of Fourier Optics and a cooled CCD sensor head. As shown in Fig. 4-3, the measurement is used in transmissive mode, where the first lens provides a Fourier transform image of the display surface. Each light beam emitted from the test area at incident angle, θ , could be focused on the focal plane at the same azimuth and at a position $x=F(\theta)$. The angular characteristics of the sample are thus measured simply and quickly, without any mechanical movement.

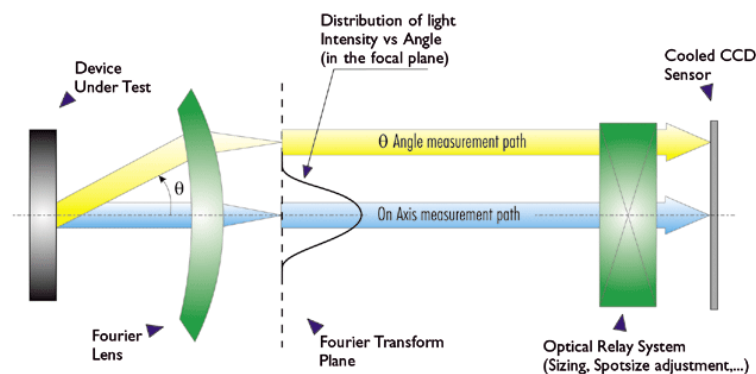


Fig. 4-3 Schematic of the conoscopic system in transmissive mode.

4.2.2 BTDF measurement device

In order to measure BTDFs of diffusive films, a light source device which can provide collimating and different-incident-angle light is required. Accordingly, we designed a device for this purpose, as shown in Fig. 4-4. Nine light-emitting diodes (LEDs) sited on the arc are chosen as the light sources. The LED is green light with a peak wavelength about 520 nm. Each LED represents each incident direction, from 0 to 80, step by every 10 degrees. Besides, the small aperture on the exit plane of LEDs and the small hole on the top plate ensure the exit light is collimated.

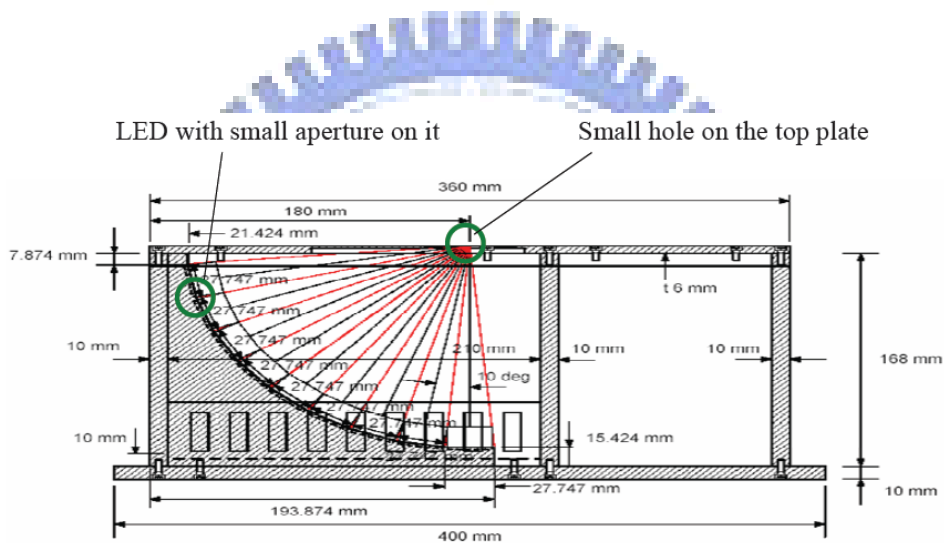


Fig. 4-4 Schematic of our designed device for BTDF measurement.

When measuring BTDFs of diffusers, the BTDF measurement device is placed under the conoscopic system to serve as the light source. The luminance information in each direction can be measured by the conoscopic system. A photograph of the experimental setting is shown in Fig. 4-5.



Fig. 4-5 Diagram of BTDF measurement.

4.3 Summary

Before the MPF fabrication, simulation software LightTools built models of backlight components to do simulations to find optimized design results. The BTDF measurement device measured the BTDF value of optical films to import into LightTools to build corresponding models. The optical property of simulation models is similar to real objects. The conoscopic system not only can measure the BRDF of the reflector but also the optical performances of backlight systems, such as angular luminance distribution, color information, et al.

To fabricate the concave-parabolic prism structure of MPFs, the idea in this thesis was to fill some material in the prism groove of conventional BEFs to be the concave-parabolic profile. Screen printing process was adopted to accomplish this idea. By adjusting the aperture ratio of the mask (screen), the amount of filled UV-curable material in the prism groove was controlled; on the other hand, different prism profiles of MPFs could be realized. Compared with the imprint method, the cost of a mask in the screen printing process is lower than that of a mold. Thus, we conclude that screen printing process has an advantage of high design flexibility to find the optimized MPF in simple process and low cost. Moreover, fabricated optimum MPF is possible to transfer to a mold for roll-to-roll mass production.

Chapter 5

Experimental results and discussions

After fabricating MPFs by screen printing process, surface profiles of fabricated MPFs were measured by a surface profiler. Then, the relationship between filling ratios and fitting curvatures of MPFs was also obtained. The experimental results, which included brightness, viewing angle, output light efficiency and real luminance images, of three experiment backlight structures (conventional, MPF and MPF-Plate case) will be presented and discussed.

5.1 Fabrication results

The optimized MPF curvature among fabricated MPFs can be obtained by measuring the surface profiles. The surface profiles between two prisms width were measured by Alpha-Step IQ^[20], as shown in Fig. 5-1. The result showed that the higher filling ratio, the flatter surface profile. In order to verify whether the fabrication result meets the designed MPF curvature, measured MPF profiles were fitted with a parabolic curve to find an approximate curvature. For example, fitted results of filling ratio 10% and 25% MPFs are shown in Fig. 5-2. Then, the relationship between filling ratio and fitting curvature of MPFs were obtained, as shown in Fig. 5-3. Among the results, the approximate curvature of filling ratio 10% MPF of 58 mm^{-1} was the closest to the optimized curvature 60 mm^{-1} of MPF and MPF-Plate case. Thus, we conclude that filling ratio 10% MPF is the optimized MPF which can suppress lamp-Mura as the conventional backlight system. In following experiments, filling ratio 10% MPF will be

adopted to do experiments for verifying our conclusion.

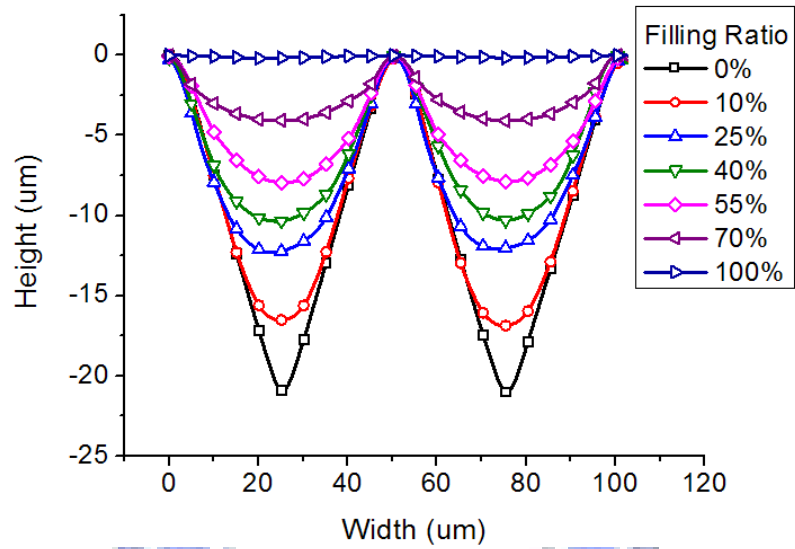


Fig. 5-1 Measured MPF surface profiles.

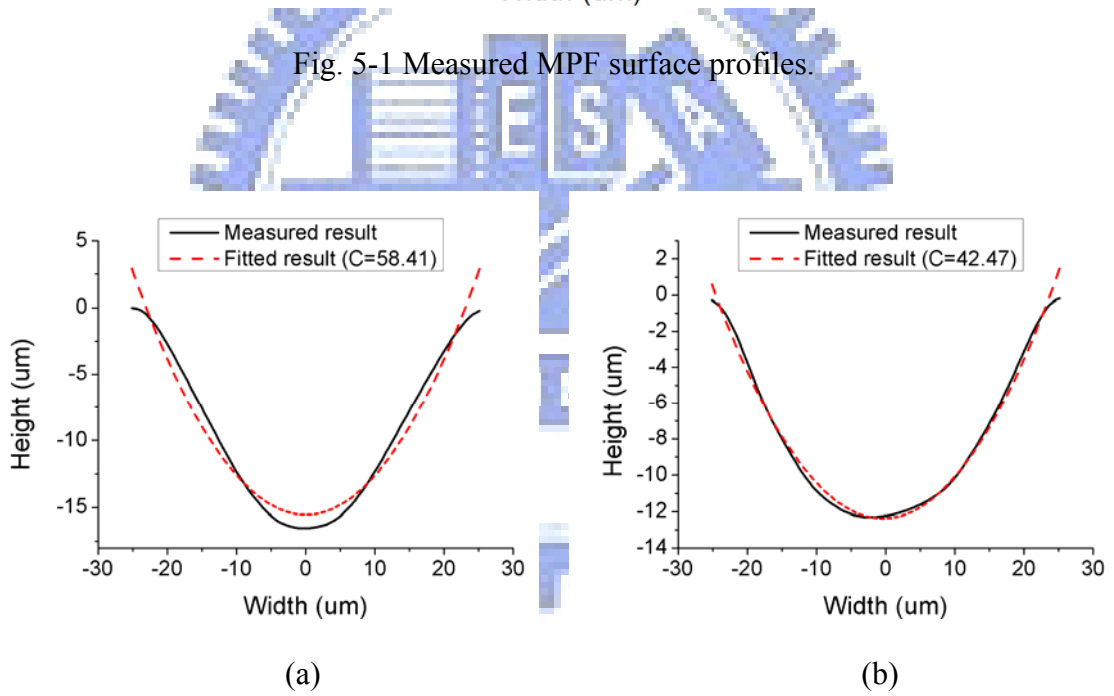


Fig. 5-2 Fitting profiles of filling ratio (a) 10% and (b) 25% MPFs.

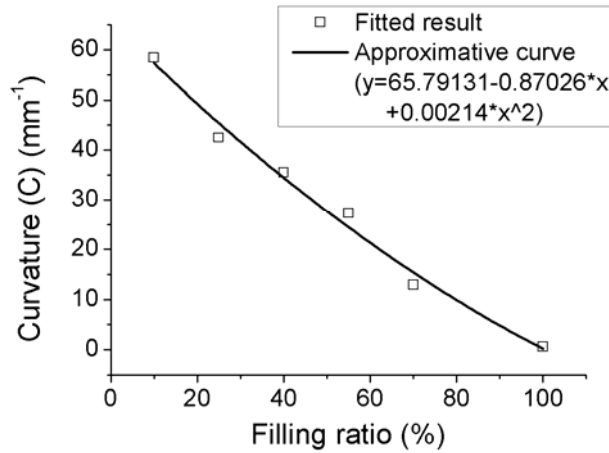


Fig. 5-3 Relationship between filling ratio and curvature.

5.2 Experimental results

Filling ratio 10% MPF was applied to MPF and MPF-Plate case to do experiments. Then, optical performances, such as lamp-Mura contrast, normal brightness, viewing angle and output light efficiency, of three experiment backlight structures (conventional, MPF and MPF-Plate case) were measured and compared.

5.2.1 Lamp-Mura contrast and average luminance of MPF case

To verify that the optimized MPF curvature had best performance of suppressing lamp-Mura, lamp-Mura contrasts of MPF case with fabricated MPFs were obtained to compare with simulation results. For the conventional backlight and MPF case, 9 points luminance between two lamps at the center of the 32" backlight system was measured by the conoscopic system, as shown in Fig. 5-4. Then, lamp-Mura contrasts were calculated according to the measured luminance distribution. The simulation and experimental results of lamp-Mura contrast and average luminance are shown in Fig. 5-5.

The lamp-Mura contrasts in the experimental and simulation results had similar trend. In

the experimental result, the filling ratio 10% MPF yielded minimum lamp-Mura contrast, 0.010, lower than the conventional backlight (0.012), which agreed with the simulation result. On the other hand, MPF case with filling ratio 10% MPF resulted in invisible lamp-Mura as the conventional backlight. Moreover, for the MPF-Plate case with the filling ratio 10% MPF, a lamp-Mura contrast, 0.018, was also obtained by experiments. However, this lamp-Mura contrast higher than the conventional does not mean that lamp-Mura is appeared. The following experimental will verify whether MPF-Plate can suppress lamp-Mura.

Moreover, the average luminance of MPF case was lower than the conventional backlight. Compared with simulation results, the average luminance of MPF case was higher than that of the conventional backlight when the curvature was below 70. The mismatch result of the average luminance will be discussed at the end of this chapter.

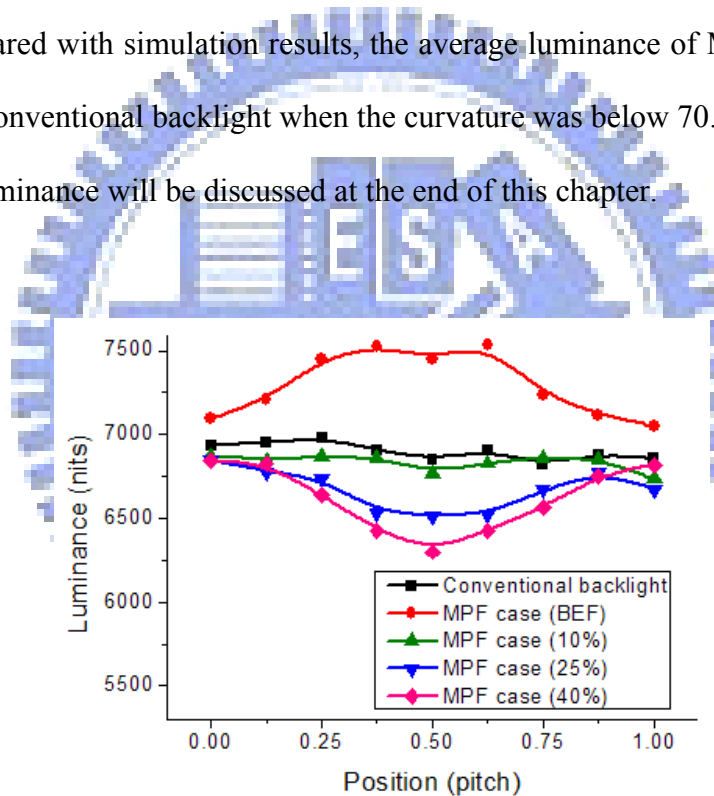


Fig. 5-4 Measured luminance distributions of conventional backlight and MPF case.

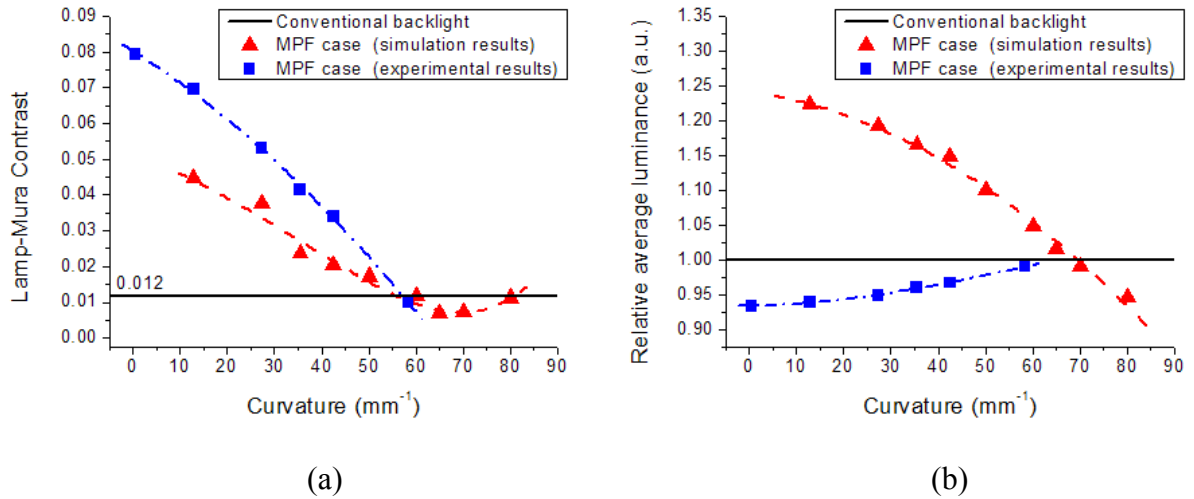


Fig. 5-5 Comparisons of simulation and experimental results in the MPF case, (a) lamp-Mura contrast and (b) relative average luminance.

5.2.2 Normal brightness and viewing angle

The experimental result of the angular luminance cross-section was measured, as shown in Fig. 5-6. Calculated values of luminance angle and of relative normal brightness are shown in Table 5-1. For MPF case, the FWHM was improved to 90° , and the normal luminance can be maintained as high as the conventional backlight. For MPF-plate case, although the normal luminance was reduced to 90% of that of the conventional backlight, the FWHM was improved further to 116° . Compared the MPF case with the MPF-Plate case, MPF case with high normal brightness is adaptable to a high brightness backlight module; MPF-Plate case with wider FWHM is suitable for a wide viewing angle LCD.

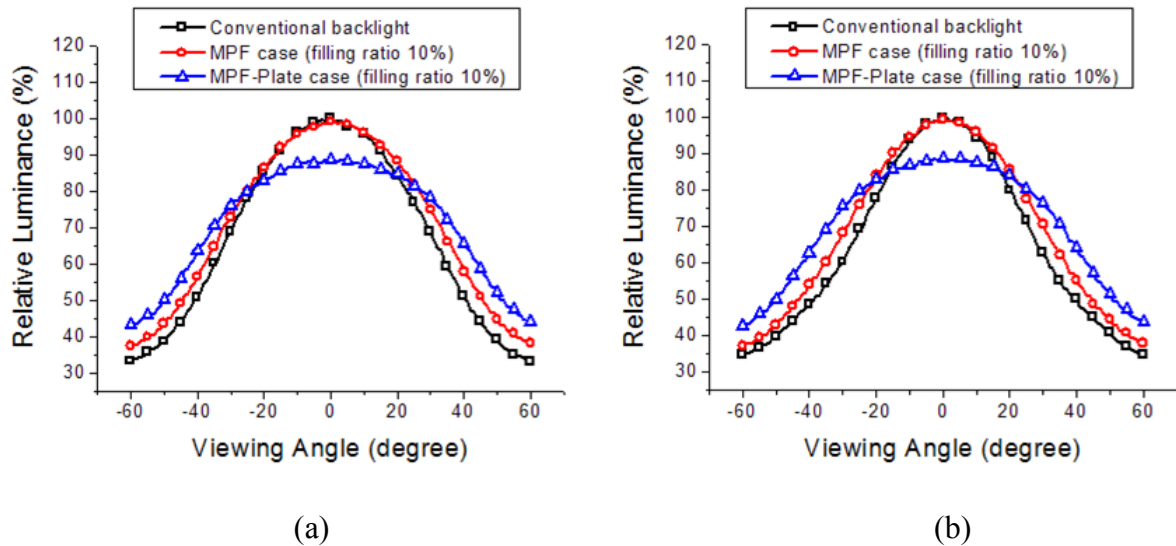


Fig. 5-6 Diagrams of luminance cross-section in (a) horizontal and (b) vertical.

Table 5-1 Relative normal brightness and luminance viewing angle.

	Conventional backlight	MPF case (filling ratio 10%)	MPF-Plate case (filling ratio 10%)
Relative Normal brightness	100%	100%	90%
FWHM@Vertical	79°	89°	116°
FWHM@Horizontal	82°	91°	116°

5.2.3 Relative output light efficiency

From the result of the angular luminance contour as shown in Fig. 5-7, the luminance viewing angles of MPF and MPF-Plate case were both wider than the conventional backlight. Consequently, for MPF and MPF-Plate case, an 8% and a 19% improvement in output light efficiency were obtained, respectively, by integrating the flux of whole viewing angles, as shown in Table 5-2. Compared with the conventional backlight and MPF case, MPF-Plate case had best performance of increasing output light efficiency. This result also verified the design motivation of MPF-Plate case.

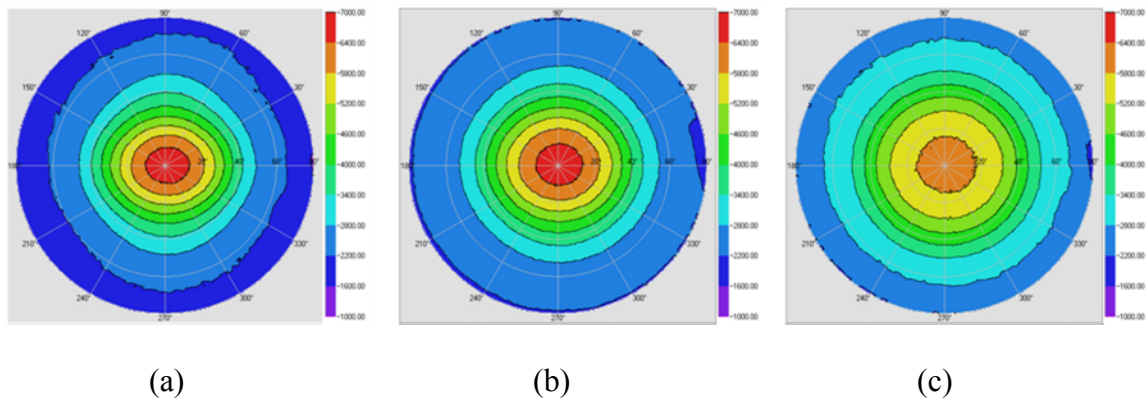


Fig. 5-7 Diagrams of angular luminance contour, (a) the conventional backlight, (b) MPF case, and (c) MPF-Plate case.

Table 5-2 Relative output light efficiency.

	Conventional backlight	MPF case (filling ratio 10%)	MPF-Plate case (filling ratio 10%)
Relative Output Light Efficiency	100%	108%	119%

5.2.4 Real luminance images

A charge-coupled device (CCD) camera (PM-1600F Color Series Imaging Photometers and Colorimeters, Radiant Imaging, Inc.^[22]) was used to record real images and contours of the output luminance distribution from backlight systems. The recorded real images are close to what the human eye sees. The captured results of three experiment cases are shown in Fig. 5-8. In the experiment, we also recorded the real image of MPF case with a conventional BEF to be a contrast with three original cases, as shown in Fig. 5-8 (b). This image had obvious lamp-Mura, and a periodic pattern was also appeared in the contour. In contrast, both MPF and MPF-Plate case had no periodic luminance pattern, therefore, they resulted in an invisible lamp-Mura image as the conventional backlight, as shown in Figs. 5-8 (a),(c), and (d). This result showed that the lamp-Mura contrast of 0.018 in the MPF-Plate case also can yield

invisible lamp-Mura. In summary, the real luminance images verified that MPF and MPF-Plate case can suppress the lamp-Mura effectively.

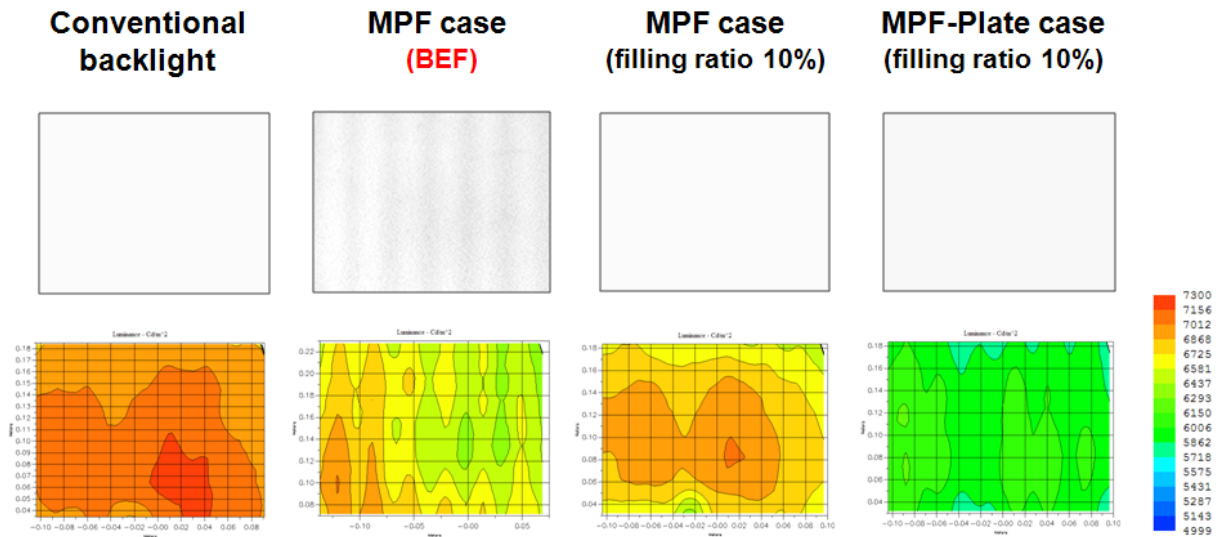


Fig. 5-8 Captured results by a CCD camera, the captured size on the backlight is 20cm by 20cm.

5.3 Summary and discussion

The optimized curvature of MPF was successfully fabricated and verified that it can suppress lamp-Mura effectively. Among fabricated MPFs of different filling ratios, the MPF filling ratio 10% of curvature 58 mm^{-1} was the closest to the optimized curvature 60 mm^{-1} of MPF and MPF-Plate case. Thus, MPF filling ratio 10% was chosen to be the optimized MPF which can suppress lamp-Mura. In MPF case, that the lamp-Mura contrast (0.010) was lower than that of the conventional backlight (0.012), agrees with the simulation result. In MPF-Plate case, the lamp-Mura contrast was 0.018, higher than 0.012. However, both MPF and MPF-Plate case resulted in an invisible lamp-Mura luminance image as the conventional backlight. Thus, we conclude the lamp-Mura contrast of 0.018 can yield invisible lamp-Mura.

Moreover, the luminance difference between simulation and experimental results of MPF case increased when MPF curvature decreased, as shown in Fig. 5-5 (b). From the optical microscope (OM) image of filling ratio 100% MPF as shown in Fig. 5-9, many particles were in the filled material. Therefore, we assume the filled UV-curable material causes the light scattering.

According to our assumption, we simulated a MPF with scattering filled material. This material was the pure UV-curable material added scattering particles (10^5 particles/mm³). In the MPF case with different curvatures, the luminance distributions with and without scattering material are shown in Fig. 5-10 (a). Additionally, the calculated result of the luminance with scattering material relative to that without is shown in Fig. 5-10 (b). Where the luminance decreased when the curvature decreased or the filling ratio increased. This result verified that the luminance is inversely proportional to the amount of scattering material.

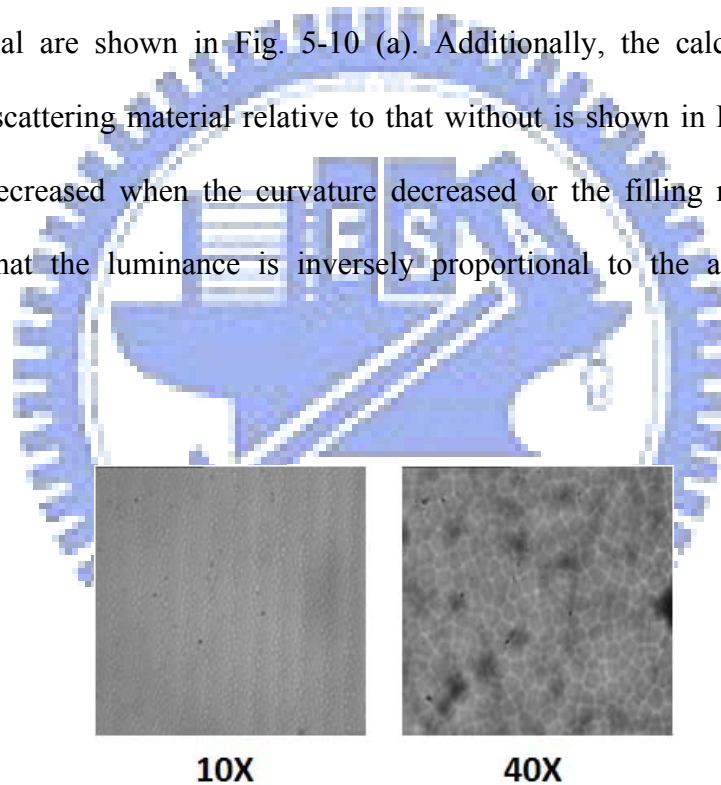


Fig. 5-9 OM pictures of filling ratio 100% MPF.

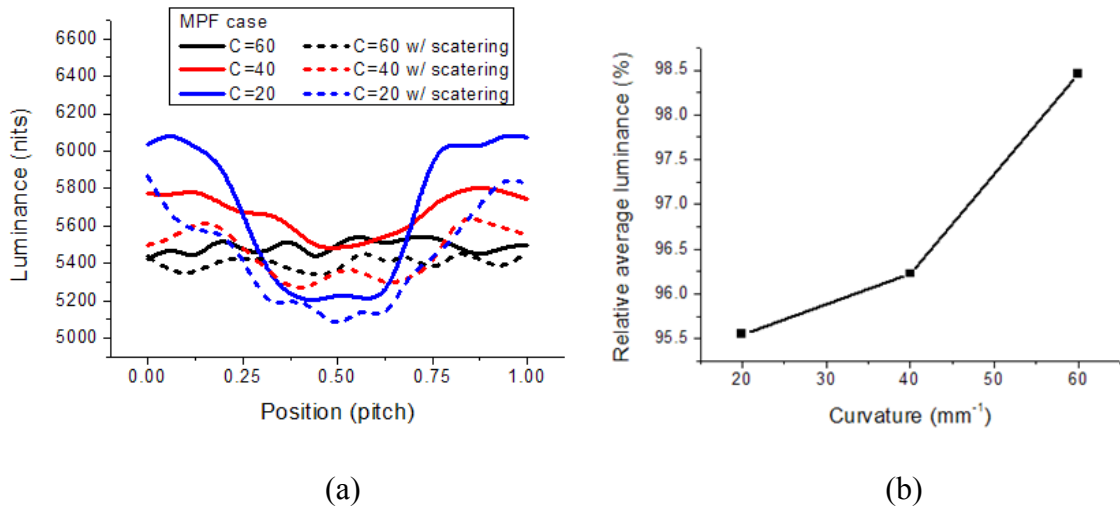


Fig. 5-10 Simulation results of (a) luminance distribution of MPF case with and without scattering filled material, (b) relative luminance of MPF case with filled material of scattering compared to that without scattering filled material.

Moreover, MPF and MPF-Plate case enhanced FWHM to 90° and 116° , respectively, in luminance viewing angle and had an 8% and a 19% improvement in output light efficiency, respectively. The higher efficiency in MPF-Plate case was also verified.

The normal luminance of MPF-Plate case is lower than that of MPF case as shown in Fig. 5-6 and Table 5-1. One possible reason is that the number of interfaces is reduced in the MPF-Plate. Because the light guiding effect exists in a pair of interfaces, the reduced number of interfaces will cause less light guiding effect and less light transferring to normal direction. Thus, MPF-Plate case had lower normal luminance than MPF case did.

Chapter 6

Patterned-MPF

A slim LCD-TV is a trend in current display market because it is suitable to mount on a wall to free up more space. However, the thickness of LCD-TV depends on the backlight structure. To achieve a slim LCD-TV, backlight thickness has to be reduced. When the backlight thickness decreases, the lamp-Mura will become more serious. Additionally, the MPF had a limitation to suppress lamp-Mura in a slim backlight system. Therefore, compared to the MPF with uniform prism structure, a Patterned-MPF was proposed to improve the uniformity in a slim backlight system.

The Patterned-MPF has various curvatures depending on the position from lamps, as shown in Fig. 6-1. This pattern concept has been applied to diffusive films for enhancing the uniformity of side-emitting backlight system by Y.-C. Lo^[23]. Because lamp-Mura is caused by a non-uniform light distribution, thus, the pattern concept can also be applied to MPF to optimize the MPF curvature at different positions. In the following designs and simulations, MPF case will be chosen to design backlight system at a thickness of 20 mm.

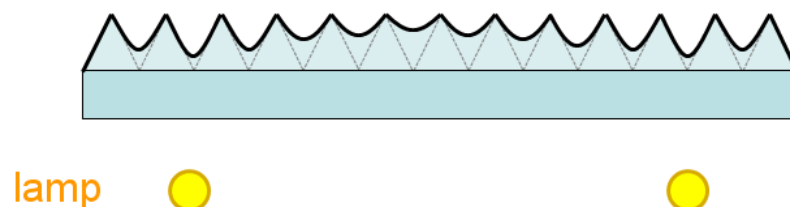


Fig. 6-1 Schematic of Patterned-MPF.

6.1 Design and simulation results

To design the curvature distribution of Patterned-MPF, luminance distributions of different MPF curvatures have to be determined first. The luminance simulation results of different thicknesses are shown in Fig. 6-2. Considering the uniformity at each position, we found output luminance is limited at 0.5 pitch. This luminance value was called the target luminance in this thesis.

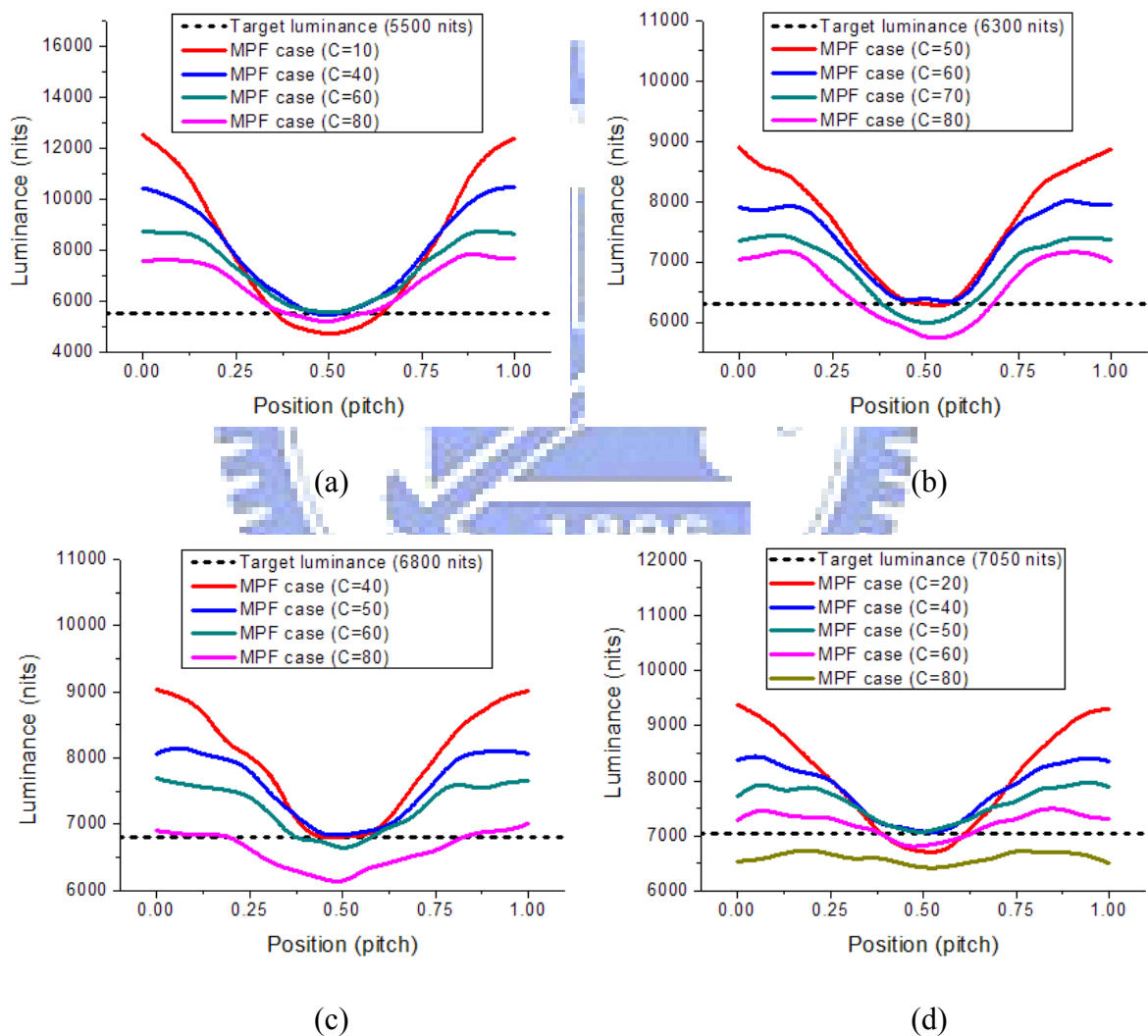


Fig. 6-2 Luminance simulation results of MPF case with different curvatures at the backlight thickness of (a) 10 mm, (b) 12 mm, (c) 14 mm, and (d) 16 mm.

The luminance at each position is designed as the same as the target, which becomes the initial curvature distribution for Patterned-MPFs, as shown in Fig. 6-3. As a result, when the thickness decreased, the variation of curvature distribution increased because of more serious lamp-Mura. In contrast, in a thick backlight system, a uniform MPF can result in a uniform light output.

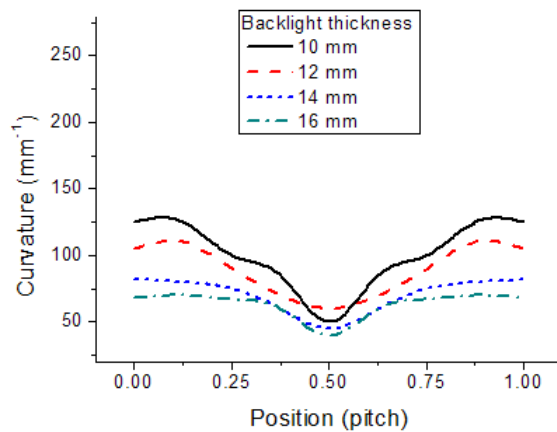


Fig. 6-3 Initial curvature distribution design of Patterned-MPF at the backlight thickness of 10 mm, 12 mm, 14 mm, and 16 mm.

The Patterned-MPF with the initial curvature distribution was then simulated to evaluate the uniformity of light output. The simulation results of output luminance distribution are shown in Fig. 6-4. The initial designed Patterned-MPFs yielded a not uniform enough luminance distribution. Therefore, the curvature distribution needs to be future modified for a more uniform light output. For example, in Fig. 6-4 (a), the luminance at 0 and 1 pitch were higher than the target luminance (5500 nits). Thus, the corresponding curvatures have to be increased for decreasing luminance. This is because the luminance of 0 or 1 pitch (above the lamp) decreased with increasing curvature, as shown in Fig. 6-2. Accordingly, the uniform light outputs (blue curves) were then yielded, as shown in Fig. 6-4, and the corresponding optimized curvature distributions are shown in Fig. 6-5.

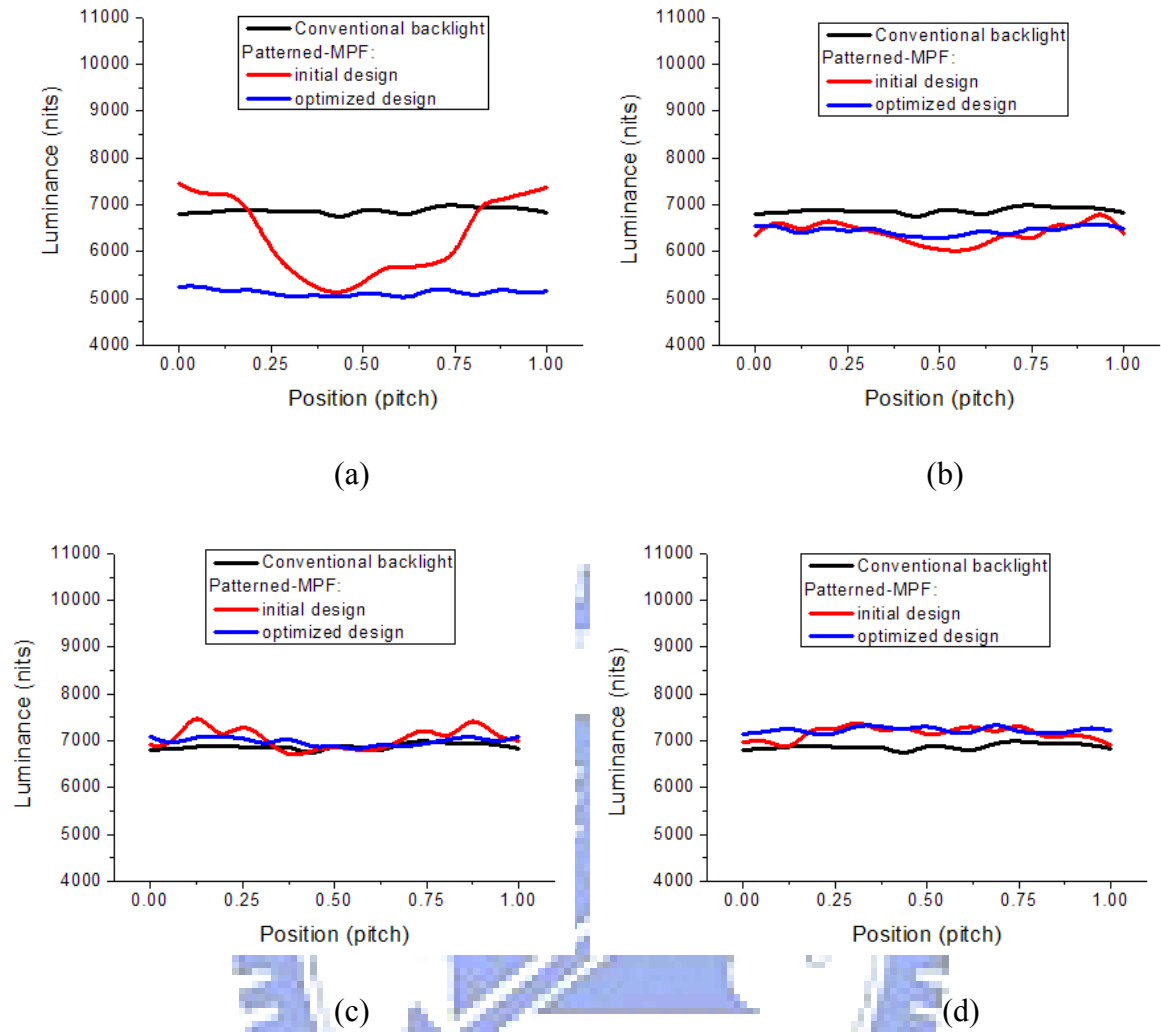


Fig. 6-4 Luminance simulation results of MPF case with designed Patterned-MPF at the backlight thickness of (a) 10 mm, (b) 12 mm, (c) 14 mm, and (d) 16 mm.

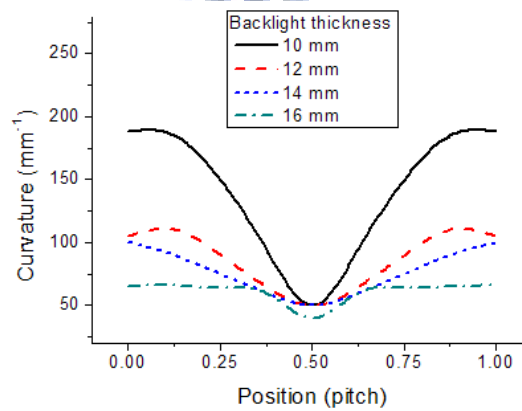


Fig. 6-5 Optimized curvature distribution design of Patterned-MPF at the backlight thickness of 10 mm, 12 mm, 14 mm, and 16 mm.

Moreover, lamp-Mura contrasts calculated from the luminance distributions in Fig. 6-4 are summarized in Table 6-1. All thicknesses using optimized Patterned-MPFs resulted in a lamp-Mura contrast smaller than 0.018 (MPF-Plate case with uniform MPF). Because the MPF-Plate case yielded invisible lamp-Mura, thus, lamp-Mura in a slim backlight system can be suppressed by optimized Patterned-MPFs. For different backlight thicknesses, the corresponding average luminance was normalized to the conventional backlight system (6875 nits), as shown in Fig. 6-6. When backlight thickness decreased, the average luminance also decreased. However, the optimized backlight thickness whose output luminance is close to that of the conventional backlight system was found about 13.3 mm.

Table 6-1 Summary of lamp-Mura contrasts in MPF case with initial and optimized Patterned-MPFs.

Thickness (mm)	Lamp-Mura contrast	
	Initial design	Optimized design
10	0.171	0.015
12	0.063	0.013
14	0.064	0.011
16	0.040	0.013

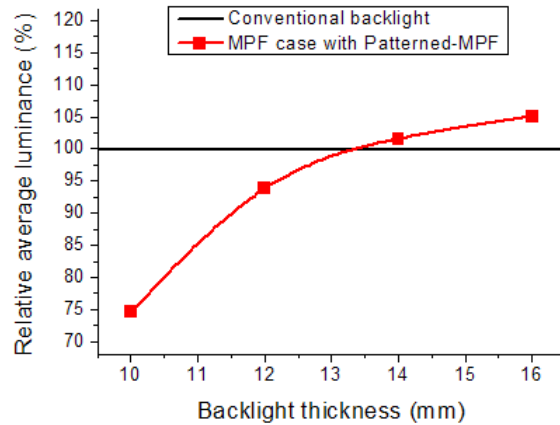


Fig. 6-6 Relationship between relative output luminance of MPF case with optimized Patterned-MPF and the backlight thickness, where the relative average luminance is normalized to the conventional backlight system (6875 nits).

6.2 Summary

In a slim backlight system, lamp-Mura becomes more serious and MPFs have a limited capability to suppress lamp-Mura. Thus, the Patterned-MPF with a variational curvature distribution was proposed to suppress lamp-Mura. According to output luminance distributions of different curvatures in MPF case, the curvature distribution was designed by assigning a target luminance value and optimized for a uniform output luminance. Then, according to the optimized curvature distribution, the optimized Patterned-MPF was designed. In the simulation results of using optimized Patterned-MPFs, the relationship between the output luminance and the backlight thickness was found. The result showed that the optimized backlight thickness of 13.3 mm resulted in an output luminance close to the conventional backlight. Thus, we conclude Patterned-MPF can be applied to MPF-Plate case for a slim, invisible lamp-Mura backlight system. Moreover, screen printing process can also be used to fabricate Patterned-MPF by a patterned-mask with corresponding aperture ratio distribution.

Chapter 7

Conclusions and future work

To display a high quality image from LCD-TVs, direct-emitting backlight systems are used to provide a sufficiently bright and uniform light source. However, direct-emitting backlight systems result in a lamp-Mura issue which adversely yields period luminance patterns to degrade the display image quality of LCDs.

In this thesis work, we developed two optical films for suppressing lamp-Mura in a direct-emitting backlight system. The ray-tracing method was used to design proposed backlight systems. Moreover, the screen printing process was adopted to fabricate proposed optical films. Compared with a general imprint process using a mold, this process is simple, lower cost, and flexible in design for different applications. In addition, the fabricated optical films are possible to transfer into a mold for roll-to-roll mass production.

7.1 Multi-performance film for suppressing lamp-Mura

Compared with BEFs, multi-performance films (MPFs) had concave-parabolic prism structures on the top surface. The concave-parabolic prism structures offered the brightness enhancement and the light scattering functions simultaneously. Thus, MPF with the scattering function could improve lamp-Mura and increase luminance viewing angle. Moreover, the output light efficiency also could be enhanced.

In this thesis, two experiment backlight structures using MPFs, MPF and the MPF-Plate case, were designed and compared with the conventional backlight of invisible lamp-Mura.

Both cases can do without a diffusive film yet, results in similar functionality. In the simulation results, for MPF case, the optimized MPF curvature range from 57 to 81 mm⁻¹ has smaller lamp-Mura contrast than the conventional backlight; for MPF-Plate case, the optimized value about 60 mm⁻¹ is the closest to the conventional backlight. Thus, the curvature 60 mm⁻¹ is the optimized value in both MPF and MPF-Plate case.

According to the fabrication results, the relationship between filling ratio and fitting curvature of MPFs were obtained. Additionally, the fabricated MPF with filling ratio 10% had the fitting curvature of 58 mm⁻¹ closed to the optimized curvature. Thus, the MPF of filling ratio 10% is the optimized MPF which can suppress lamp-Mura effectively.

To verify whether lamp-Mura can be suppressed by the MPF with optimized curvature, the MPF of filling ratio 10% was then applied to MPF and MPF-Plate. In the lamp-Mura contrast result, the value of MPF case was 0.010 smaller than 0.012 (conventional backlight), but that of MPF-Plate case was 0.018 higher. However, according to real luminance images and contours, the MPF and MPF-Plate case with filling ratio 10% MPF can result in invisible lamp-Mura. Thus, the lamp-Mura contrast of 0.018 also can yield invisible lamp-Mura.

From the measurement results, MPF and MPF-Plate case enhanced luminance viewing angle to 90° and 116° FWHM and had an 8% and a 19% improvement in the output light efficiency, respectively. Additionally, the results revealed that the MPF-Plate case can enhance more output light efficiency than the MPF case. The experimental results of the three experiment backlight structures are summarized and compared in Table 7-1. Both MPF and MPF-Plate case with optimized filling ratio 10% MPF successfully achieved higher quality display image with suppressed lamp-Mura, and they also enhanced the luminance viewing angle and output light efficiency.

Table 7-1 Comparison of experimental results between the conventional backlight, MPF case, and MPF-Plate case.

	Relative normal brightness	FWHM viewing angle	Relative output light efficiency	Lamp Mura	Cost
Conventional backlight	□ (100%)	□ (80°)	□ (100%)	○	□
MPF case (filling ratio 10%)	□ (100%)	○ (90°)	○ (108%)	○	○
MPF-Plate case (filling ratio 10%)	△ (90%)	◎ (116°)	◎ (119%)	○	○

◎: very good / ○: good / □: normal / △: bad

7.2 Patterned multi-performance film for slim backlight systems

For achieving a slim backlight system, a slim backlight is necessary. When the backlight thickness was reduced, the lamp-Mura is more serious. Moreover, MPF has a limited capability to suppress lamp-Mura in a slim backlight system.

Accordingly, the Patterned-MPF which has variational curvature distribution is proposed to suppress lamp-Mura. Considering the uniformity at each position, the curvature distribution was optimized for a uniform output luminance. Then, the Patterned MPFs with the optimized curvature distribution was designed. In the MPF case using Patterned-MPFs, the relationship between the output luminance and the backlight thickness was found. This result showed that the optimized backlight thickness was about 13.3-mm which yielded output luminance closed to that of the conventional backlight.

In conclusion, Patterned-MPF was designed to reduce the backlight thickness and to suppress lamp-Mura simultaneously. Additionally, we conclude Patterned-MPF also can be applied to MPF-Plate case for a slim, compact, suppressed lamp-Mura backlight system.

7.3 Future work

Patterned-MPF also can be designed to further do without the bottom diffuser for lower backlight cost. To realize Patterned-MPFs in slim backlight systems, a patterned mask with corresponding aperture ratio distribution has to be designed and fabricated. In addition, compared with CCFLs, light-emitting diodes (LEDs) have some advantages such as low power consumption and small volume. Thus, LED backlight systems will replace CCFL ones and become the mainstream backlight product in the future. Because the LED backlight system has a hotspot issue, the light output distribution is non-uniform. We think MPF can be further extended to a 2-D concave paraboloid structure to apply to LED backlight systems for improving the backlight uniformity. One possible kind of 2-D MPF is concave-quadrangular pyramid, as shown in Fig. 7-1. The screen-printing process also can be utilized to fabricate the concave paraboloid structures of 2-D MPF. Thus, MPF is also a candidate to apply for next generation LED backlight systems of low cost and high optical performance.

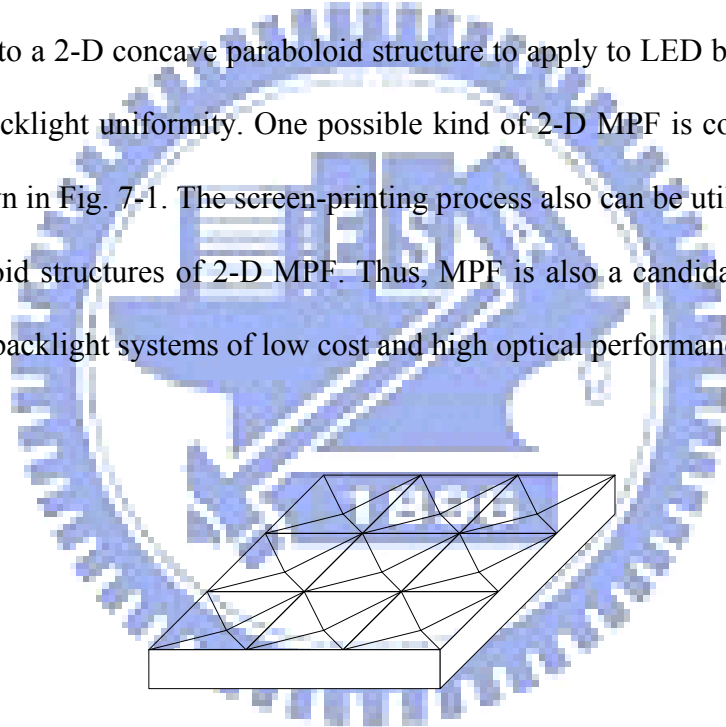


Fig. 7-1 Concave-quadrangular pyramid structure of 2-D MPF.

Reference

- ¹ E. Lueder, *Liquid Crystal Displays*, John Wiley& Sons, p.294 (2000)
- ² E. Lueder, *Liquid Crystal Displays*, John Wiley& Sons, p.121 (2000)
- ³ J. Graf, G. Olczak, M. Yamada, D. Coyle and S. Yenug, “ BACKLIGHT FILM & SHEET TECHNOLOGIES FOR LCDs,” Seminar Lecture Note, SID’08, p.M-12/6 (2008)
- ⁴ 邱正茂、賴詩文和賴宏仁, ”LCD-TV 背光源的發展現況 – 誰能勝出”, 工業材料雜誌, 221 期, p.72-86, 2005 年 5 月
- ⁵ J. C. Pan and A. Lin, “Emerging Technologies for Backlight Modules,” IDMC, p.463-466 (2007)
- ⁶ M. Schiavoni, G. Counil, P. Gayout, J.-L. Allano and R. Marandon, “5.4: Novel Glass Diffuser Plate for Large LCD-TV” SID’07 DIGEST, p.50-53 (2007)
- ⁷ L. M. Seon, O. Y. Sik, P. D. Sung, K. S. Yoon and L. J. Yeal, “Optimum Design Characteristics of a Direct Type Backlight Unit,” IDW’06, p.921-924 (2006)
- ⁸ C.-C. Kang, J.-F. Lin, M.-C. Chen and P.-R. Wang, “An Innovative Solution for the Thinness of Backlight Units with the Implementation of Transflectors,” IDMC’07, p.685-688 (2007)
- ⁹ J.-C. Hsieh, Y.-P. Huang, C.-H. Chen, Y.-C. Lo, J.-Y. Fang, H.-P. D. Shieh, G.-S. Yu and T. Chiang, “P-111: Multi-Performance Film (MPF) for Highly Efficient LCD Backlights,” SID’08 DIGEST, p.1606-1609 (2008)
- ¹⁰ Emphasis Materials, Inc., <http://www.EmphasisMaterials.com>
- ¹¹ Optical Research Associates, <http://www.opticalres.com/>
- ¹² W. J. Smith, *Modern Optical Engineering*, McGraw-Hill, p.4 (2001)
- ¹³ E. Hecht, *Optics*, Addison Wesley, p.101 (2002)

-
- ¹⁴ E. Hecht, *Optics*, Addison Wesley, p.98 (2002)
- ¹⁵ E. Hecht, *Optics*, Addison Wesley, p.122 (2002)
- ¹⁶ W. J. Smith, *Modern Optical Engineering*, McGraw-Hill, p.6 (2001)
- ¹⁷ W. J. Smith, *Modern Optical Engineering*, McGraw-Hill, p.8 (2001)
- ¹⁸ A. Prat and M. I. Rahmi, "19-3: Glass Diffuser for LCD TV Backlight," EuroDisplay, p.347-350 (2002)
- ¹⁹ 3 M company, <http://www.3m.com/>
- ²⁰ An-Chi Wei, "Planar Optics and its Application to Display," PhD thesis, p.19, NCTU (2007)
- ²¹ <http://www.kla-tencor.com/j/servlet/Product?prodID=14>
- ²² <http://www.radiantimaging.com/>
- ²³ Y.-C. Lo, J.-Y. Fang, Y.-P. Huang, H.-P. D. Shieh, G.-S. Yu and T. Chiang, "A Novel Patterned Diffuser for High Uniform and High Bright LCD Backlights," IDMC'07, p.642-645 (2007)

